

WIDE RANGE TUNABLE TRANSCONDUCTANCE FILTERS

Except where reference is made to the work of others, the work described in this thesis is my own or was done in collaboration with my advisory committee. This thesis does not include proprietary or classified information.

Matthew Anderson

Certificate of Approval:

John Y. Hung
Professor
Electrical and Computer Engineering

Bogdan M. Wilamowski, Chair
Professor
Electrical and Computer Engineering

Thaddeus A. Roppel
Associate Professor
Electrical and Computer Engineering

Joe F. Pittman
Interim Dean
Graduate School

WIDE RANGE TUNABLE TRANSCONDUCTANCE FILTERS

Matthew Anderson

A Thesis

Submitted to

the Graduate Faculty of

Auburn University

in Partial Fulfillment of the

Requirements for the

Degree of

Master of Science

Auburn, Alabama

May 10, 2008

WIDE RANGE TUNABLE TRANSDUCTANCE FILTERS

Matthew Anderson

Permission is granted to Auburn University to make copies of this thesis at its discretion, upon the request of individuals or institutions and at their expense. The author reserves all publication rights.

Signature of Author

Date of Graduation

VITA

Matthew Anderson, the son of Phillip and Cathy Springfield, was born on May 23, 1983. Upon graduating Summa cum Laude in Electrical Engineering at Auburn University in Spring 2006 he accepted a job at Archangel Systems Inc., also in Auburn. Since graduation he has worked under his advisor, Dr. Bogdan Wilamowski, to complete the requirements for the Masters program.

THESIS ABSTRACT

WIDE RANGE TUNABLE TRANSCONDUCTANCE FILTERS

Matthew Anderson

Master of Science, May 10, 2008
(B.S., Auburn University, 2006)

62 Typed Pages

Directed by Bogdan Wilamowski

Generation of filters using operational transconductance amplifiers and capacitors (OTA-C) has become more and more popular over recent years. This is due to the need for high quality analog filters that can be implemented on a standard CMOS integrated circuit. While operational amplifier based active filters have served this purpose in the past, the OTA-C filter has advantages over a classic amplifier design. A simple yet effective method of analytical synthesis was developed that makes use of ladder circuits, which are widely understood. Given the ladder circuit of a filter of any order, an equivalent OTA-C filter can be easily synthesized. The synthesis process is shown for both a low pass prototype filter, and its band pass transformation. Higher order filters can easily be synthesized by extending the design process described. An OTA was developed which was designed specifically to address the complications involved in implementing filters with high quality factors. The design of a band pass filter is then implemented in CMOS with the OTA to show the effect of non-ideal elements. The CMOS filter implementation is capable of achieving

a quality factor of 20 up to frequencies of 100 kHz. The reference current can be used to tune the filter center frequency linearly over three decades. This flexibility in center frequency tuning can be used to compensate for process variations or for creating general purpose filters with constant passive element values.

ACKNOWLEDGMENTS

I would like to express my deepest appreciation to my advisor, Dr. Wilamowski. Without his patience and guidance I would not be in the position I am today. From him I have learned a multitude of things, of which, engineering is only the tip of the iceberg.

Style manual or journal used Journal of Approximation Theory (together with the style known as “aums”). Bibliography follows van Leunen’s *A Handbook for Scholars*.

Computer software used The document preparation package T_EX (specifically L^AT_EX) together with the departmental style-file `aums.sty`.

TABLE OF CONTENTS

LIST OF FIGURES	x
1 INTRODUCTION	1
1.1 Motivation	1
1.2 Thesis Outline	3
2 TRANSCONDUCTANCE FILTERS	5
2.1 Low Pass Filter Synthesis	5
2.1.1 LC Ladder Circuit	5
2.1.2 OTA-C Transformation	6
2.2 Band Pass Filter Synthesis	8
2.2.1 LC Ladder Circuit	8
2.2.2 OTA-C Transformation	10
3 OTA'S IMPLEMENTED IN VLSI	14
3.1 Approach	14
3.2 Implementation	14
3.2.1 Differential Pair OTA	14
3.2.2 Mirrored Cascode OTA	18
3.2.3 Mirrored Cascode OTA With Improved Current Mirror	21
4 TUNABLE FILTERS IN VLSI	27
4.1 Implementation of Low Pass Filter	27
4.2 Implementation of Band Pass Filter	30
4.3 Implementation of Higher Order Filter	35
5 CONCLUSION	43
BIBLIOGRAPHY	45
APPENDICES	47
A SPICE LEVEL 7 NMOS MODEL FOR AMIS 0.5 μm PROCESS	48
B SPICE LEVEL 7 PMOS MODEL FOR AMIS 0.5 μm PROCESS	50

LIST OF FIGURES

2.1	Low pass filter LC implementation	5
2.2	Frequency response of 3 rd order prototype Chebyshev LPF	7
2.3	Low pass filter OTA implementation with input and termination resistances	9
2.4	Low pass filter OTA implementation without input and termination resistances	10
2.5	Band pass filter ladder circuit	11
2.6	Frequency response of 3 rd order prototype Chebyshev BPF	13
2.7	3 rd order prototype Chebyshev BPF OTA implementation	13
3.1	Simple OTA implementation	15
3.2	Transconductance vs reference current for the OTA shown in Figure 3.1	16
3.3	Output Resistance vs reference current for the OTA shown in Figure 3.1	16
3.4	OTA with Cascode current mirror	18
3.5	Transconductance vs reference current for the OTA shown in Figure 3.4	19
3.6	Output Resistance vs reference current for the OTA shown in Figure 3.4	19
3.7	AC sweep of transconductance for OTA in Figure 3.4	20
3.8	Two input OTA implementation	23
3.9	Transconductance vs reference current for the OTA shown in Figure 3.8	24
3.10	Output Resistance vs reference current for the OTA shown in Figure 3.8	24

3.11	AC sweep of transconductance for OTA in Figure 3.8	25
3.12	Output current verses differential input voltage for Iref=5 nA	26
4.1	Third order Chebyshev low pass filter with F_c of 1 kHz	28
4.2	Third order Chebyshev low pass filter for five reference currents	29
4.3	Reference current vs LPF critical frequency	30
4.4	Third order Chebyshev band pass with $F_c = 1$ kHz, Q=1	32
4.5	Third order Chebyshev band pass with $F_c = 1$ kHz, Q=20	33
4.6	Exploded view of third order Chebyshev band pass filter with $F_c = 1$ kHz, Q=20	34
4.7	Third order Chebyshev band pass filter for four reference currents	36
4.8	Reference current vs BPF center frequency	37
4.9	5 th order band pass filter ladder circuit	38
4.10	5 th order prototype Chebyshev BPF OTA implementation	38
4.11	Fifth order Chebyshev band pass filter centered at 10 kHz	40
4.12	Third order Chebyshev band pass filter centered at 10 kHz	41
4.13	Fifth order Chebyshev band pass filter ranging 1 kHz to 10 kHz	42

CHAPTER 1

INTRODUCTION

1.1 Motivation

The Operational Transconductance Amplifier (OTA) finds a wide range of uses in the field of analog electronics. Over the past two decades, it has become increasingly popular as a building block in analog filters. These OTA capacitor (OTA-C) filters have several advantages over the more typical operational amplifier configurations. These advantages include:

- **Fully Integrated Implementation:** To create a quality fully integrated filter a few design constraints must be added. For instance, it is a benefit to have only grounded capacitors in the filter design. There are two reasons for this design constraint; most importantly, grounded capacitors can be implemented in a smaller area than their floating counterparts. Also, grounded capacitors reduce the impact of shunt capacitances that can seriously affect the final transfer function.
- **Electronic Filter Tuning:** Because the transconductance (g_m) of an OTA is used as a design parameter, the filter response can be modified by changing the g_m of various OTA's. In practice this can be accomplished with a tuning current or voltage that sets the bias level of the OTA. Electronic tuning is necessary to overcome process variations. As an added bonus, if the filter

center frequency can be varied over a wide band, a generally designed filter can find use in many applications.

- **High Frequency Operation:** Although not addressed in detail in this work, it is a fact that the design of a high frequency OTA is more easily accomplished than a high frequency operational amplifier. This is due to the fact that the OTA does not require the output stage of a typical operational amplifier. Even with the second order effects that must be considered, bandpass filters have been reported that can operate in the gigahertz range.

Despite their advantages, OTA-C filters are often overlooked by design engineers because they are not well understood. They are perceived as hard to design because literature on the subject is often either ambiguous or unnecessarily complicated. In this work, transconductance filters are introduced and explained from the point of view of the passive ladder filter circuit. The ladder point of view is preferred because of its popularity and ease of design [2]. Two main techniques exist in the literature to transform a ladder circuit into its OTA-C implementation and they have been shown to be theoretically equivalent [4]. The first technique, known as element replacement, involves using capacitors directly and substituting inductors with an equivalent circuit that has an inductive input impedance. The other method is referred to as operational simulation, or signal flow graph method. In operational simulation, the node voltages and mesh currents of the ladder circuit are simulated by summations and the ladder

elements are simulated by integration operators. For the purposes of this paper the operational simulation method will be used because of its ease of understanding from a set of state equations or transfer function.

A bulk of research has been dedicated to lower order OTA-C filter structures [5] - [6]. This research is done with the idea that low order sections can be used to build high order filters. One problem with this approach is the loss of generality. Once a second order section is built as a design block, all implementable transfer functions are based on that block. Another problem is the sensitivity of these blocks to element values. Since the design assumes each section is identical, any difference in element values can have serious impacts on the filter response. A better approach is to develop equations for the circuit to be implemented, and match those equations with only the OTA and capacitors as building blocks. In this way any order ladder circuit can be synthesized. Less research is devoted to this concept [8] - [9], and as such it is the crux of this work.

1.2 Thesis Outline

In the early chapters, ideal OTA's will be used to support the theory of the filter synthesis. Chapter 2 will introduce the process and show examples of a low pass and band pass prototype. Chapter 3 will show the OTA design process. The design will start with a simple OTA and motivations for improving the OTA will be discussed. The final OTA design will be developed in SPICE using CMOS 0.5 μm technology. Finally, in Chapter 4, the CMOS OTA will be substituted for the ideal one to show

the non-ideal effects. In the simpler case of the low pass filter, the non-ideal impacts will be minor. However, band pass filters with high quality factors can tax even the most carefully designed amplifiers.

CHAPTER 2

TRANSCONDUCTANCE FILTERS

2.1 Low Pass Filter Synthesis

2.1.1 LC Ladder Circuit

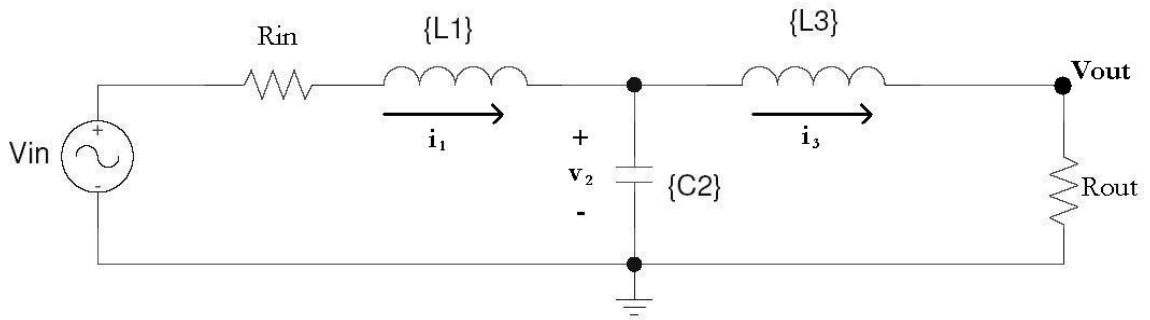


Figure 2.1: Low pass filter LC implementation

The implementation of a third order Chebyshev low pass filter is sufficient to show the design process. The ladder circuit for such a filter, designed for minimum capacitance, is shown in Figure 2.1. For simplicity, values for the passive elements are chosen to set the cut-off frequency at 1 Hz and are shown in table 2.1. The element values were calculated using Matlab software written for ladder circuits [3]. The frequency response of such a circuit is shown in Figure 2.2.

Element	Capacitance
L1	0.352 F
C2	0.173 F
L3	0.352 F

Table 2.1: Capacitor values for low pass filter prototype

2.1.2 OTA-C Transformation

Using the current and voltage conventions defined in Figure 2.1, one can easily write the state space equations for this particular circuit. In this case the state variables have been chosen such that each state variable corresponds to the output of an OTA.

$$\begin{aligned}
\dot{i}_1 &= \frac{1}{L_1}(V_{in} - R_{in}i_1 - v_2) \\
\dot{v}_2 &= \frac{1}{C_2}(i_1 - i_3) \\
\dot{i}_3 &= \frac{1}{L_3}(v_2 - R_{out}i_3)
\end{aligned} \tag{2.1}$$

The transfer function generated from this system of equations is

$$\frac{V_{out}}{V_{in}} = \frac{R_{out}}{L_1C_2L_3s^3 + (L_1C_2R_{out} + C_2L_3R_{in})s^2 + (C_2R_{in}R_{out} + L_1 + L_3)s + R_{in} + R_{out}} \tag{2.2}$$

If the equations shown in equation set (2.1) are used to implement an OTA-C filter, the circuit would be as shown in Figure 2.4. Analyzing the circuit in Figure 2.4 with the OTA output voltages as state variables, the state equations become those

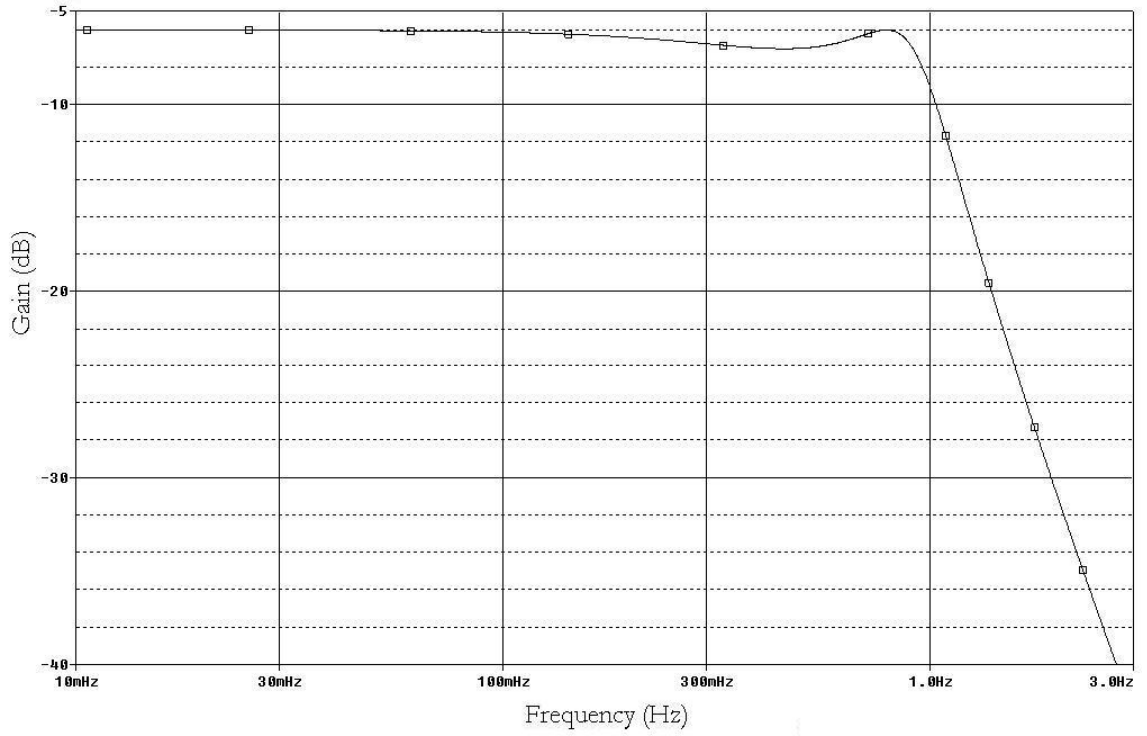


Figure 2.2: Frequency response of 3rd order prototype Chebyshev LPF

shown in equation set (2.3) assuming an equal transconductance for each OTA. The corresponding transfer function is shown in (2.4).

$$\begin{aligned}
 \dot{v}_1 &= \frac{g_m}{L_1}(V_{in} - v_1 - v_2) \\
 \dot{v}_2 &= \frac{g_m}{C_2}(v_1 - v_3) \\
 \dot{v}_3 &= \frac{g_m}{L_3}(v_2 - v_3)
 \end{aligned} \tag{2.3}$$

$$\frac{V_{out}}{V_{in}} = \frac{g_m^3}{L_1 C_2 L_3 s^3 + (L_1 C_2 + C_2 L_3) g_m s^2 + (C_2 + L_1 + L_3) g_m^2 s + 2g_m^3} \quad (2.4)$$

The comparison of equations (2.2) and (2.4) reveals some interesting consequences of the OTA-C implementation. First, the passive component values (capacitors) must be scaled by the value of g_m to achieve the same filter critical frequency. Secondly, the transfer function no longer depends on R_{in} and R_{out} . This can best be explained by observing that an OTA with negative feedback works as a resistor. If there is a resistor in the feedback path, as in R_{in} and R_{out} , its value does not impact the output voltage because the output current will change with the resistance. For a large load, as would be the case for an operational amplifier input, R_{in} and R_{out} can be replaced with shorts.

Figure 2.3 shows the OTA-C circuit using a four input OTA where necessary. Using ideal components in SPICE, the frequency response of the circuit is exactly the same as the LC ladder response shown in Figure 2.2. This is to be expected since, at least for the ideal case, the two transfer functions are equivalent.

2.2 Band Pass Filter Synthesis

2.2.1 LC Ladder Circuit

Using the standard ladder circuit filter transformations, it is easy to determine the bandpass filter corresponding to the low pass filter from the previous section.

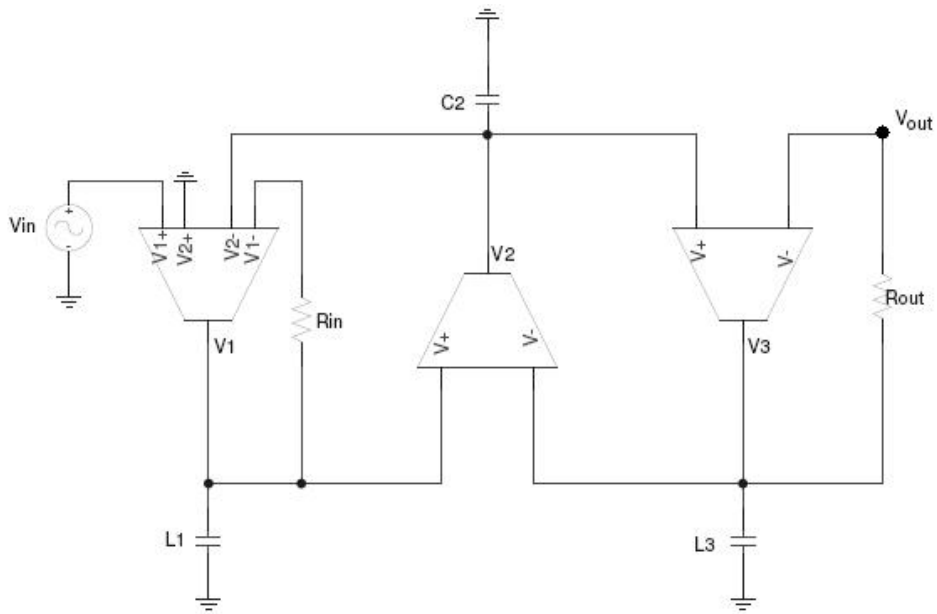


Figure 2.3: Low pass filter OTA implementation with input and termination resistances

This is the circuit shown in Figure 2.5. As before, the values of the elements have been chosen to obtain a center frequency of 1 Hz. The frequency response for this filter is shown in Figure 2.6.

Element	Capacitance
L1	0.322 F
C1	0.079 F
L2	0.160 F
C2	0.158 F
L3	0.322 F
C3	0.079 F

Table 2.2: Capacitor values for band pass filter prototype

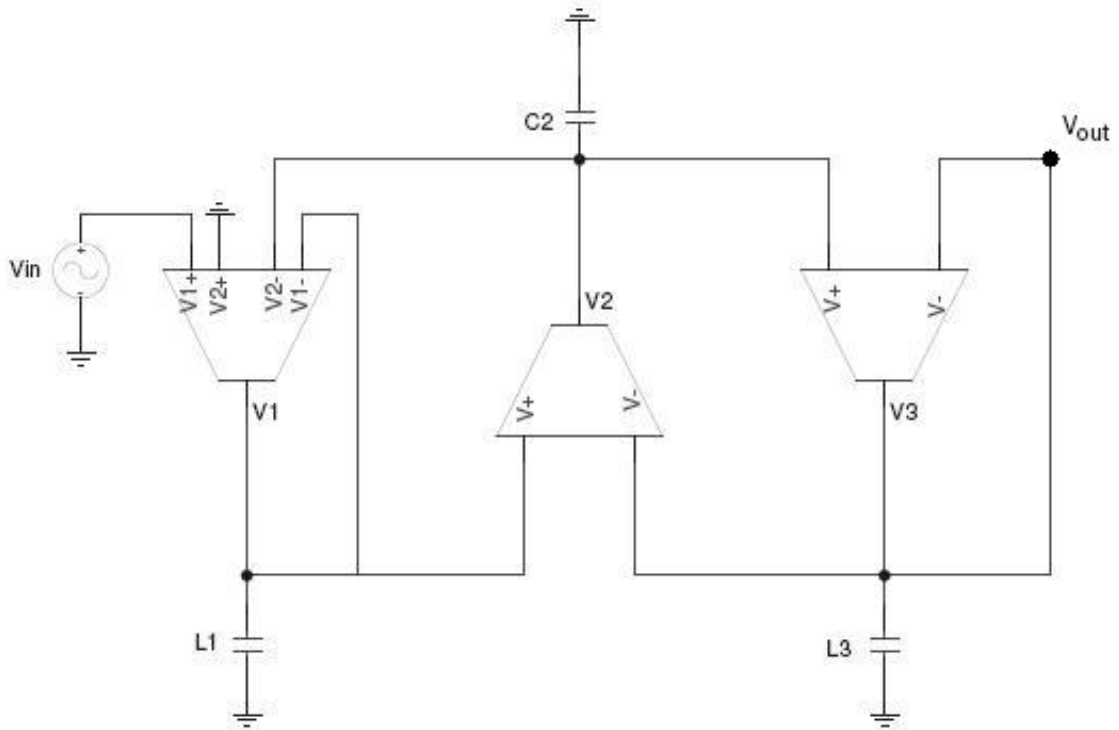


Figure 2.4: Low pass filter OTA implementation without input and termination resistances

2.2.2 OTA-C Transformation

One can write the circuit equations as before using the same type of conventions on Figure 2.5. These results are shown in equation set (2.5).

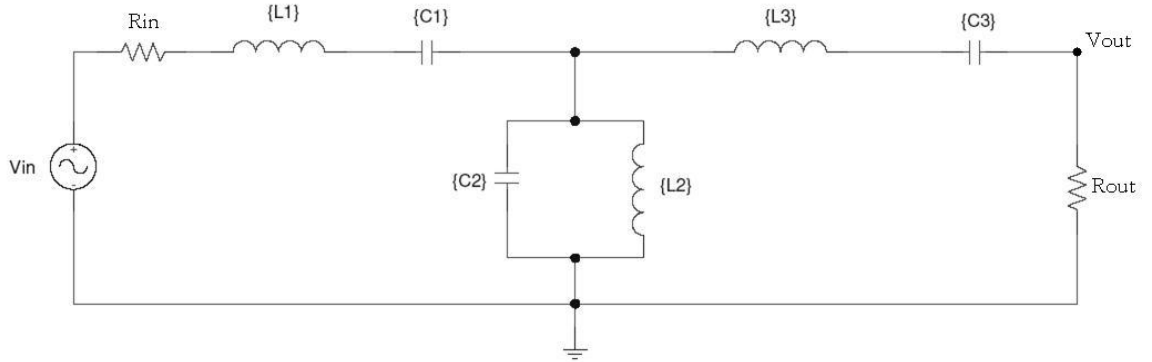


Figure 2.5: Band pass filter ladder circuit

$$\begin{aligned}
 \dot{i}_1 &= \frac{1}{L_1}(V_{in} - i_1 R_{in} - v_2 - v_4) \\
 \dot{v}_2 &= \frac{1}{C_1}(i_1) \\
 \dot{i}_3 &= \frac{1}{L_2}(v_4) \\
 \dot{v}_4 &= \frac{1}{C_2}(i_1 - i_3 - i_5) \\
 \dot{i}_5 &= \frac{1}{L_3}(v_4 - v_6 - i_5 R_{out}) \\
 \dot{v}_6 &= \frac{1}{C_3}(i_5)
 \end{aligned} \tag{2.5}$$

However, the band pass filter presents a slightly more complicated situation than the low pass. The difficulty arises from the equation for \dot{i}_1 . Although one can easily fabricate a four input OTA, it will obviously have two positive inputs and two negative inputs. Using the equations from equation (2.5) will result in the OTA corresponding to \dot{i}_1 needing three negative inputs. To remedy this situation, it is necessary to

manipulate the signs of the variables. It can be clearly seen that if v_2 were positive in the equation for \dot{i}_1 then a standard four input OTA could be used in the circuit. This being the case, changing the sign of v_2 everywhere it occurs in equation set 2.5 results in equation set 2.6. Clearly, this solution is not unique.

$$\begin{aligned}
 \dot{i}_1 &= \frac{1}{L_1}(V_{in} - i_1 R_{in} + v_2 - v_4) \\
 \dot{v}_2 &= \frac{1}{C_1}(-i_1) \\
 \dot{i}_3 &= \frac{1}{L_2}(v_4) \\
 \dot{v}_4 &= \frac{1}{C_2}(i_1 - i_3 - i_5) \\
 \dot{i}_5 &= \frac{1}{L_3}(v_4 - v_6 - i_5 R_{out}) \\
 \dot{v}_6 &= \frac{1}{C_3}(i_5)
 \end{aligned} \tag{2.6}$$

The idealized circuit corresponding to equation set (2.6) is shown in Figure 2.7 with R_{in} and R_{out} replaced with shorts. As in the case of the low pass circuit, the filter response is exactly the same as show in Figure 2.6.

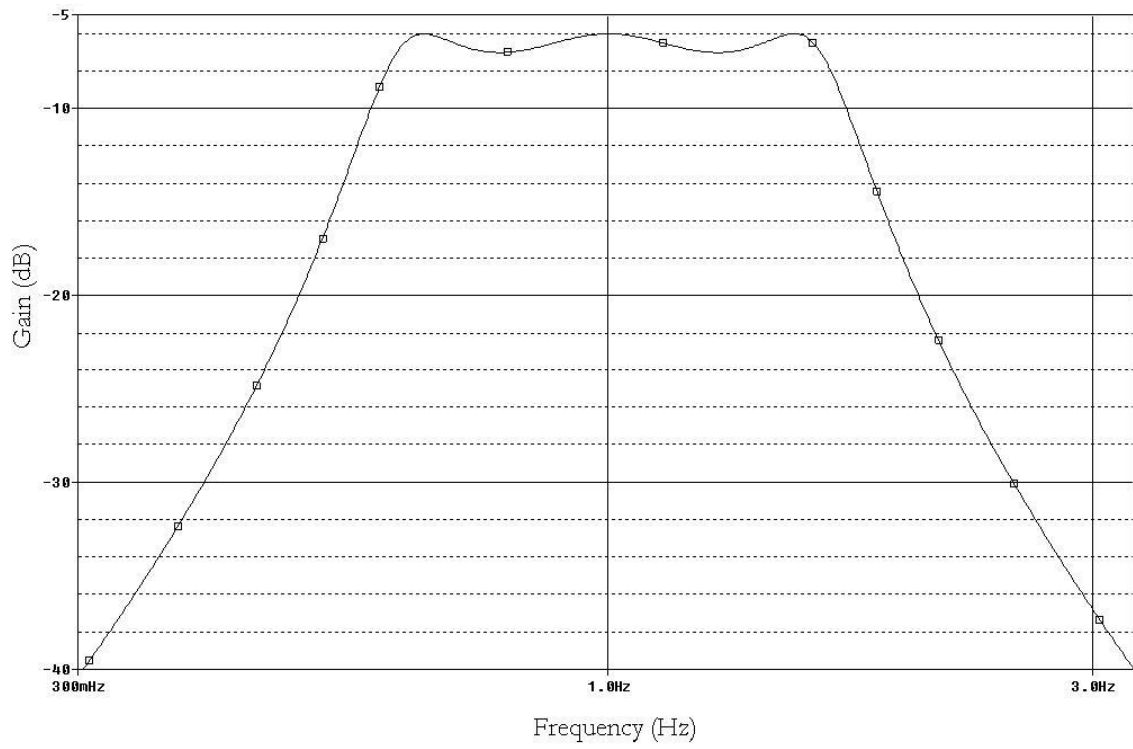


Figure 2.6: Frequency response of 3rd order prototype Chebyshev BPF

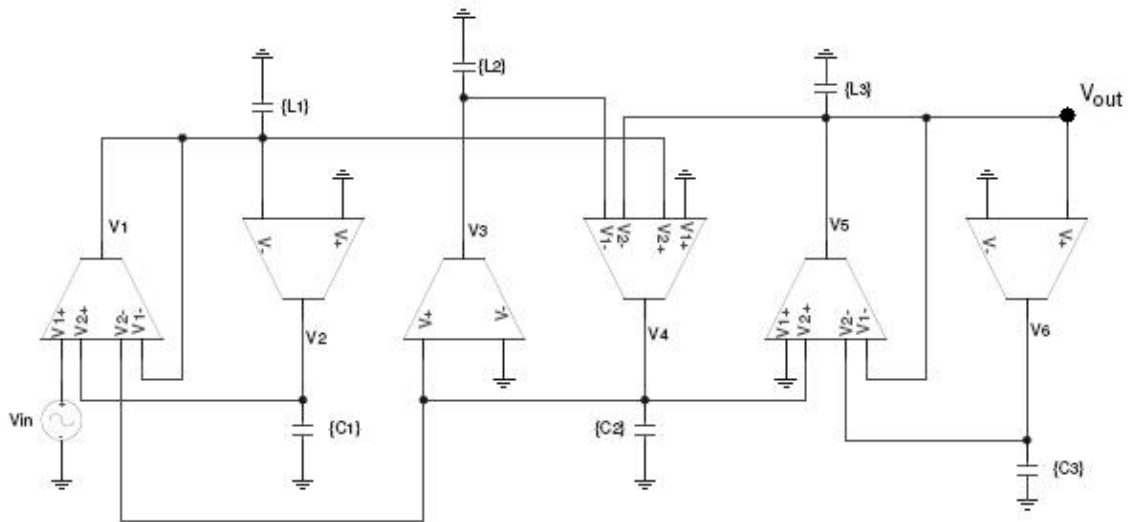


Figure 2.7: 3rd order prototype Chebyshev BPF OTA implementation

CHAPTER 3

OTA'S IMPLEMENTED IN VLSI

3.1 Approach

When implementing an OTA in VLSI it is important to consider the end use of the circuit. This is done in order to decrease the non-ideal characteristics of the OTA that are most significant to the end application. In the case of the filter application, the finite output resistance of the OTA can seriously degrade the shape of the desired filter, especially at higher quality factors [12]. Due to this fact, high output impedance must be a focus in the OTA design process.

Another necessary consideration that results from the filtering application is the question of tuning. It is clear from the transfer functions derived in Chapter 2 that the critical frequency of the filter will change linearly with transconductance. Therefore, it is advantageous to derive a method of tuning transconductance linearly. If this is accomplished, adjustments for process variations are much easier to implement.

3.2 Implementation

3.2.1 Differential Pair OTA

The simplest implementation of a two input OTA is a differential pair like the one shown in Figure 3.1. The current at the output node, I_{out} , depends on the difference in the two input voltages and the transconductance is determined by transistor M_1 (or

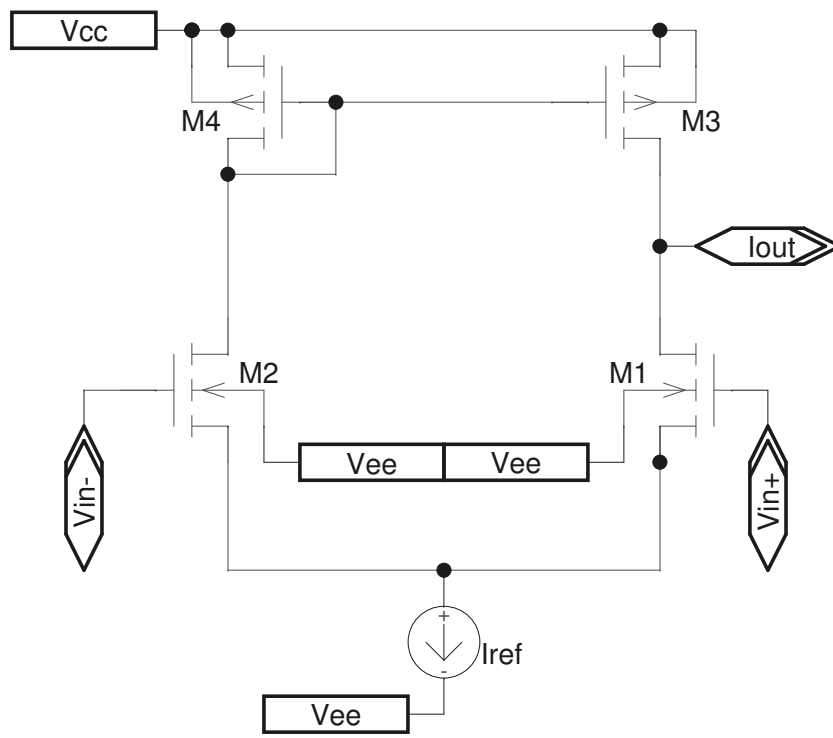


Figure 3.1: Simple OTA implementation

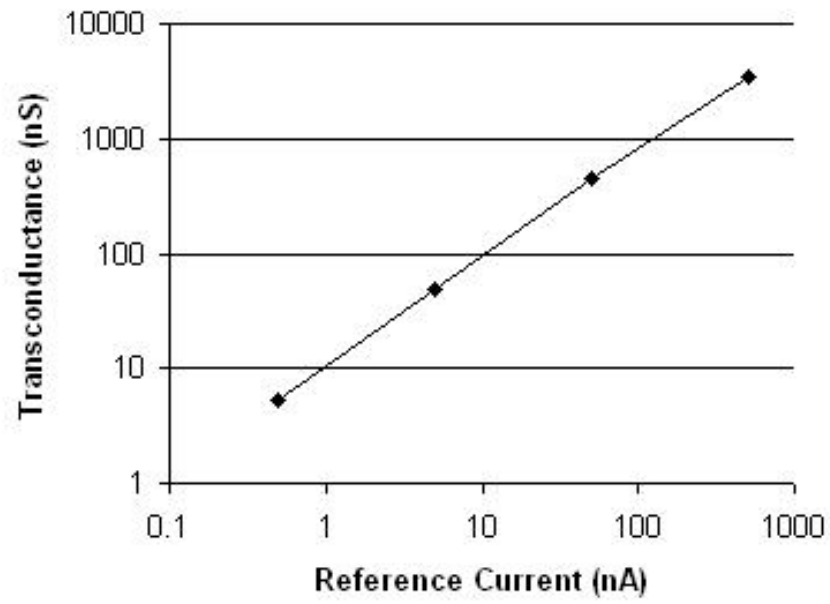


Figure 3.2: Transconductance vs reference current for the OTA shown in Figure 3.1

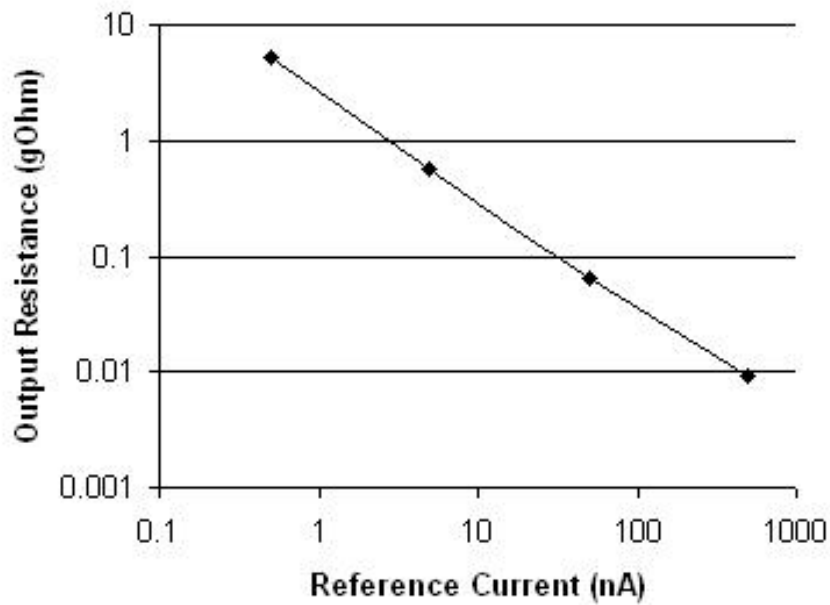


Figure 3.3: Output Resistance vs reference current for the OTA shown in Figure 3.1

M_2). Simulating in SPICE using $0.5 \mu\text{m}$ process models, transconductance varies with current as shown in Figure 3.2. The input transistors are operated in subthreshold conduction. This is done to keep transconductance linearly tunable and to achieve larger output resistances. If the amplifier were operated outside the subthreshold conduction region, the transconductance would be described by equation (3.1).

$$g_m = \sqrt{2K_n I_d} \quad (3.1)$$

However, in subthreshold conduction the transconductance follows equation (3.2), where η in this case is around two.

$$g_m = \frac{I_d}{\eta V_t} \quad (3.2)$$

The drawback is that the amplifier will not work as well at higher frequencies. However, to achieve higher quality factors the tradeoff is necessary. For filter design, a large transconductance value is not as important as a large output resistance. Figure 3.3 shows how the output resistance of the differential pair varies with bias current which follows equation (3.3).

$$R_{out} = r_{o-pmos} \parallel r_{o-nmos} \quad (3.3)$$

Even for the smallest bias currents, the output resistance is marginal. A more advanced design must be considered for filtering applications.

3.2.2 Mirrored Cascode OTA

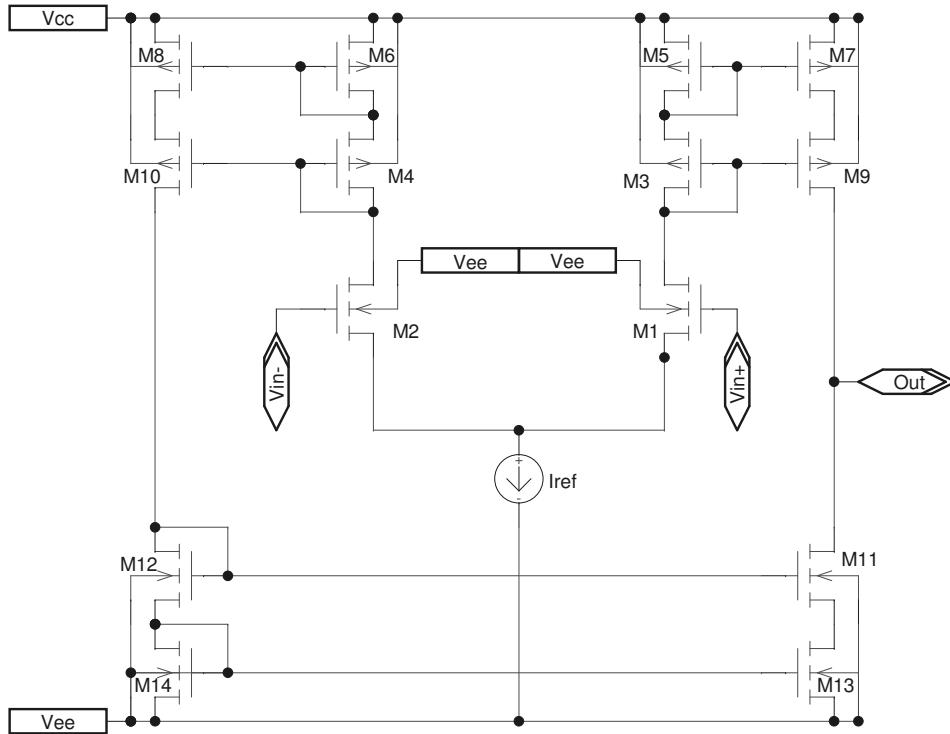


Figure 3.4: OTA with Cascode current mirror

A cascode structure is a good next step since higher output impedances can be obtained without sacrificing transconductance. The OTA structure in Figure 3.4 is a mirrored cascode [13], with the mirror being a cascode current mirror. The operation of the circuit is similar as before, but this time the currents produced by the input transistors are both mirrored to the output. This lets the output resistance of the

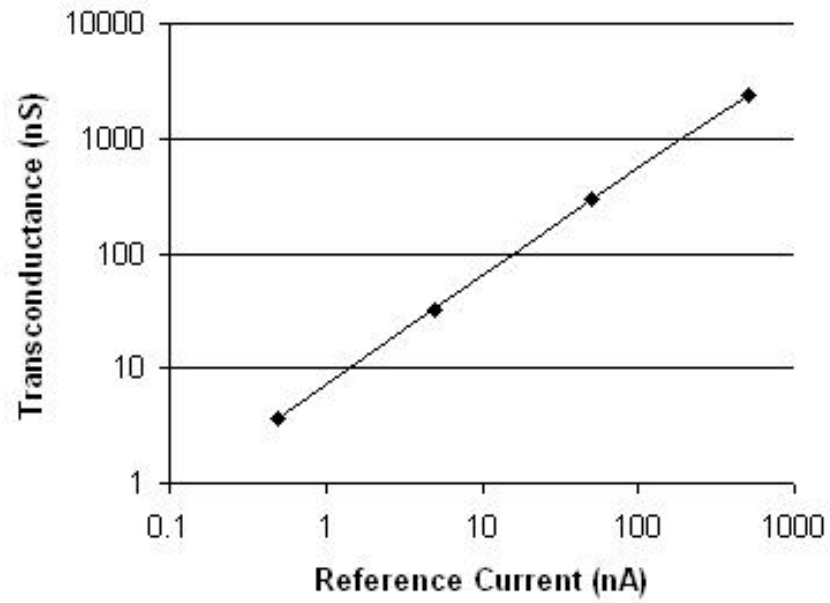


Figure 3.5: Transconductance vs reference current for the OTA shown in Figure 3.4

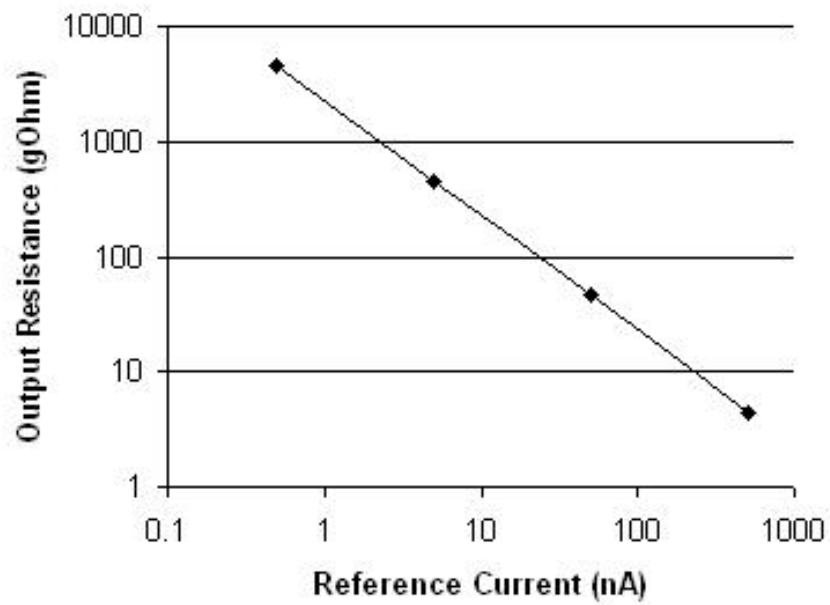


Figure 3.6: Output Resistance vs reference current for the OTA shown in Figure 3.4

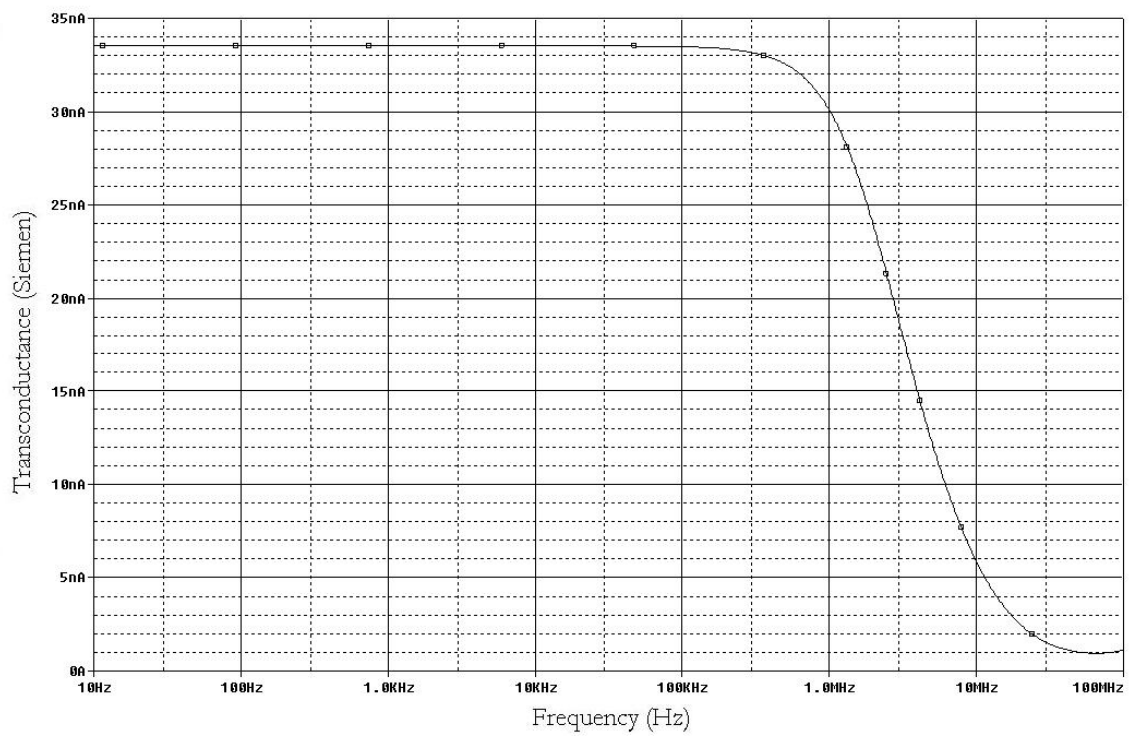


Figure 3.7: AC sweep of transconductance for OTA in Figure 3.4

OTA match that of the current mirror which is described by equation (3.4).

$$R_{out} = r_{o-nmos} \left(1 + \frac{r_{o-nmos}}{r_{m-nmos}}\right) \parallel r_{o-pmos} \left(1 + \frac{r_{o-pmos}}{r_{m-pmos}}\right) \quad (3.4)$$

Figure 3.5 shows the simulation results for transconductance closely resemble those shown for the simpler differential pair. However, Figure 3.6 indicates that the output resistance has increased by a factor of a thousand.

Although the mirrored cascode OTA will perform adequately in a filter applications [14], improvements can still be made. The drawback of using cascode architectures in OTA design comes from the impact of the non-dominant poles. In the case of the mirrored cascode, the non-dominant poles of interest are located at the input side of the current mirrors [13]. If the non-dominant poles are too close to the dominant pole, the filter transfer function can be distorted at higher quality factors or higher frequencies [12]. Figure 3.7 shows a plot of the transconductance versus frequency. The constant roll off shown indicates the non-dominant poles are very close to the dominant one.

3.2.3 Mirrored Cascode OTA With Improved Current Mirror

To push out the non-dominant poles, an attempt must be made to decrease capacitances at the nodes of interest. In this case, this occurs at the input sides of the current mirrors. The cascode current mirrors used in Figure 3.4 have two gate capacitances connected connected to the input node of the current mirror. The

frequency response could be improved if only one gate capacitance was necessary to achieve the same output resistance. This problem can be solved with an improved current mirror. The current mirror chosen, presented by Zeki and Kuntman, is known as IAFCCM [10]. Figure 3.8 shows the mirrored cascode circuit implementing the IAFCCM. Figures 3.9 and 3.10 show the simulation results for the circuit. The transconductance is about the same as before, and the output resistance is actually improved by a factor of ten. However, the main impact of the improved design is shown in Figure 3.11. The frequency response of the OTA is improved, but more importantly, the non-dominant pole is pushed to higher frequencies.

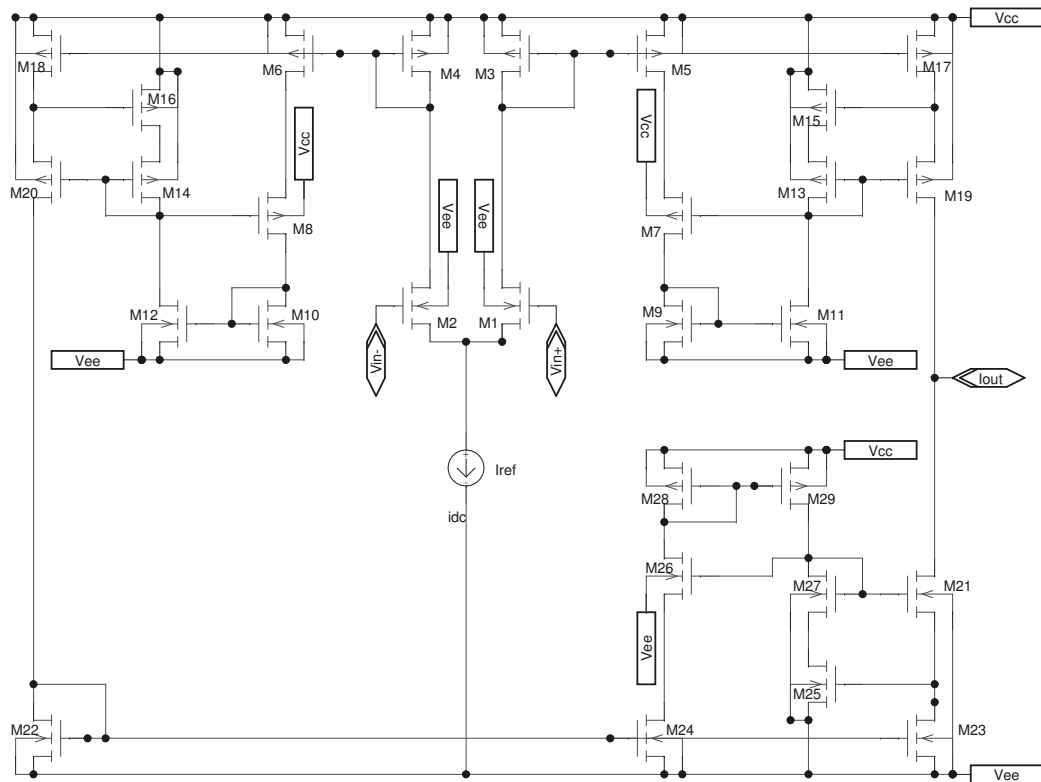


Figure 3.8: Two input OTA implementation

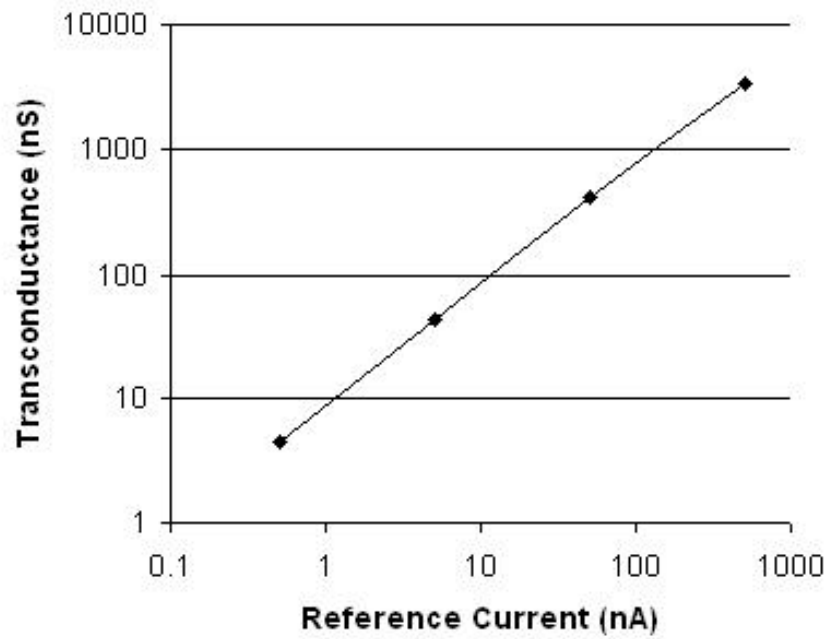


Figure 3.9: Transconductance vs reference current for the OTA shown in Figure 3.8

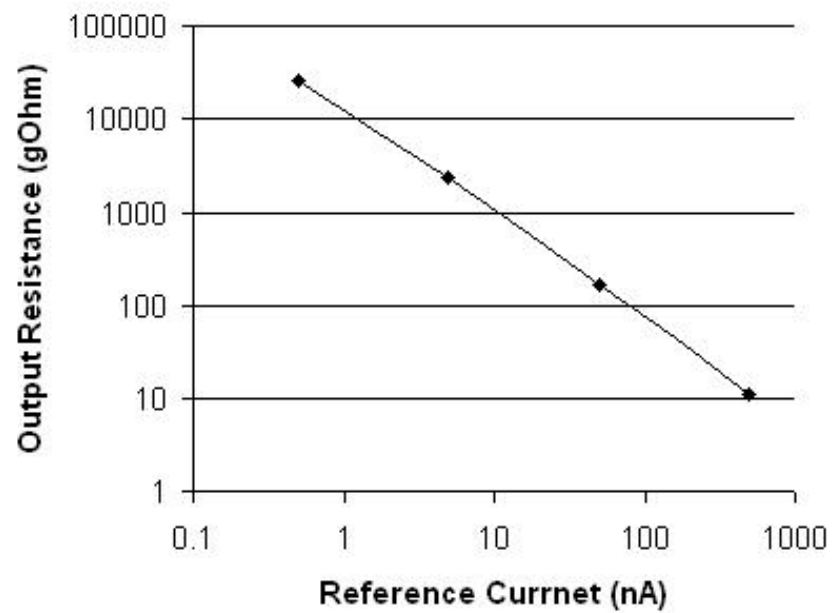


Figure 3.10: Output Resistance vs reference current for the OTA shown in Figure 3.8

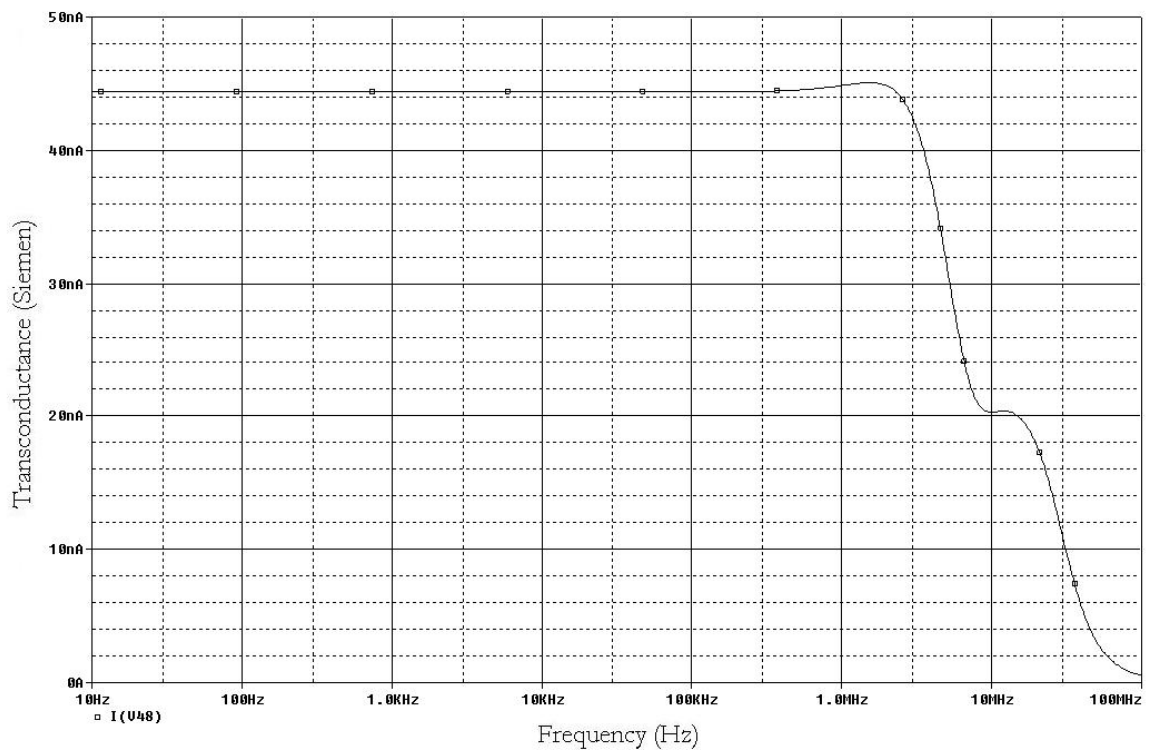


Figure 3.11: AC sweep of transconductance for OTA in Figure 3.8

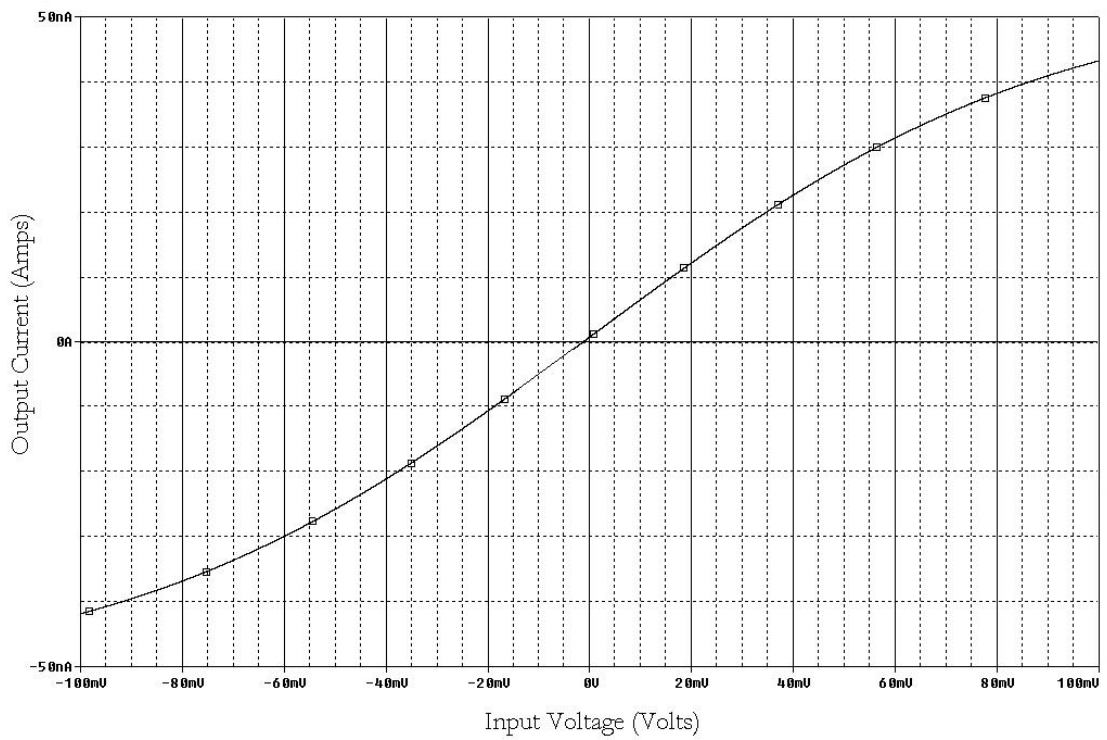


Figure 3.12: Output current verses differential input voltage for $I_{ref}=5$ nA

CHAPTER 4
TUNABLE FILTERS IN VLSI

4.1 Implementation of Low Pass Filter

The low pass filter prototype developed in section 2.1 will now be implemented using the OTA developed in section 3.2.3. The prototype was developed for a critical frequency of 1 Hz and assuming a transconductance of 1 S. Therefore, the passive elements must be scaled to account for more realistic OTA transconductances as well as higher critical frequencies. The values shown in table 4.1 were chosen to produce a critical frequency of 1 kHz at a reference current of 0.5 nF. These values were calculated using equation (4.1) with G_m equal to the OTA transconductance at 0.5 nF, 6.92 nS, and F_{new} equal to the desired critical frequency, 1 kHz.

$$C_{new} = \frac{C_{prototype} * G_m}{F_{new}} \quad (4.1)$$

The frequency response of this filter can be seen in Figure 4.1. Other than the critical frequency, the response is identical to the ideal one presented earlier in Figure 2.2.

Element	Capacitance
L1	2.43 pF
C2	1.19 pF
L3	2.43 pF

Table 4.1: Capacitor values for low pass filter

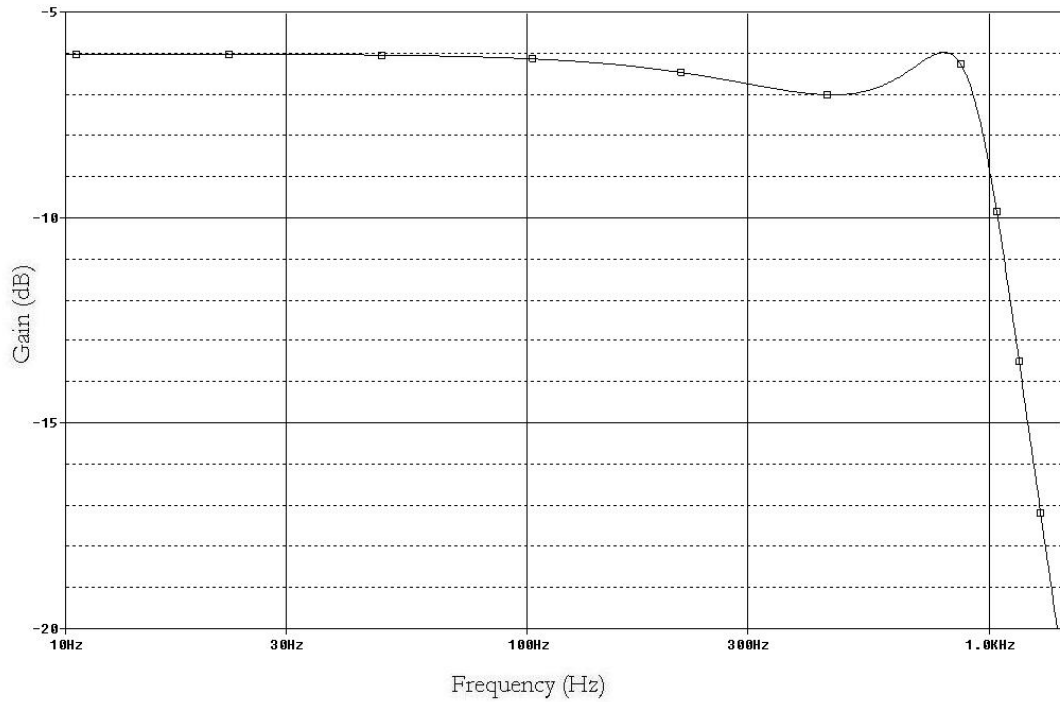


Figure 4.1: Third order Chebyshev low pass filter with F_c of 1 kHz

Since the transconductance of each OTA helps determine the transfer function of the filter, the reference currents can be used to change the filter characteristics. There are many benefits to this flexibility. For one, the individual currents of each OTA can be adjusted to compensate for errors in the capacitor values caused by process variations. On the other hand, if all the OTA reference currents are changed together, the result is a shift in the filter's critical frequency. Figure 4.2 shows the same filter for increasing values of reference current.

It is clear that many applications would benefit from the ability to change filter critical frequencies quickly and easily. For instance, the designed filter can sweep the

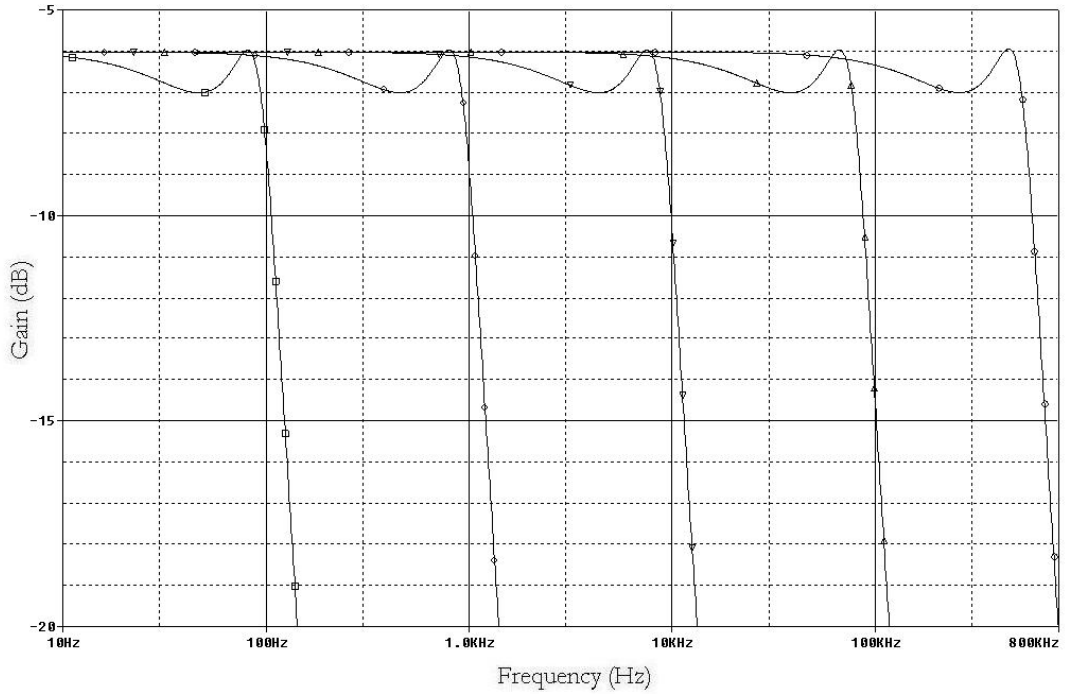


Figure 4.2: Third order Chebyshev low pass filter for five reference currents

entire range of audio frequencies with a simple change of reference current. Figure 4.2 indicates that the low pass filter critical frequency can be placed anywhere between 10 Hz and 600 kHz without adjusting passive element values. For much of this range, filter critical frequency depends linearly on the reference current. Figure 4.3 shows a plot of reference current verses critical frequency for the filters shown in Figure 4.2. The linearity degrades only slightly at the reference current extremes. Linearity can only be maintained for certain biasing conditions of the input transistors of the OTA. In other words, there is a trade-off between the range of the filter and the linearity of the critical frequency tuning. On the plus side, as reference current increases so does

the maximum operating frequency of the OTA. This allows the filter to consume only the amount of power necessary to operate at a given frequency.

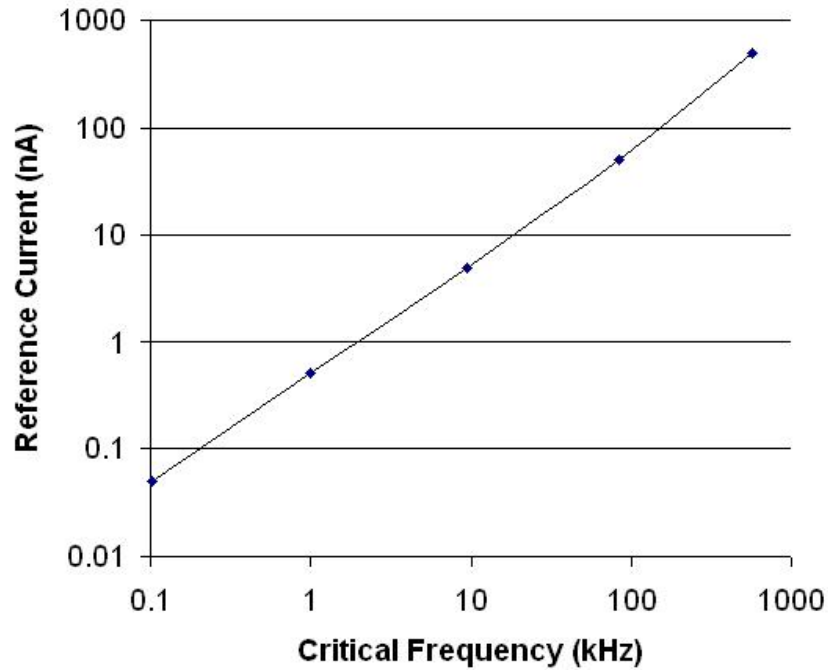


Figure 4.3: Reference current vs LPF critical frequency

4.2 Implementation of Band Pass Filter

Due to its added complexity, the band pass filter implementation will show more clearly the differences between the VLSI implementation and the ideal. As was the case with the low pass filter, the elements must once again be scaled based on the frequency and transconductance. However, with the band pass filter the quality factor must also be considered when choosing the element values. For a quality factor of 1, equation (4.1) can still be used. If designed to have a center frequency of 1 kHz at a

Element	Capacitance
L1	21.13 pF
C1	5.16 pF
L2	10.38 pF
C2	10.50 pF
L3	21.13 pF
C3	5.16 pF

Table 4.2: Capacitor values for band pass filter with Q=1

reference current of 5 nA, equation (4.1) yields the capacitances shown in table 4.2. Simulating with these capacitances results in the frequency response shown in Figure 4.4.

To design for higher quality factors, the equations for capacitor values must be revised to those shown in equation set (4.2).

$$\begin{aligned}
L_{1new} &= \frac{L_{1prototype} * G_m * Q}{F_{new}} \\
C_{1new} &= \frac{C_{1prototype} * G_m}{F_{new} * Q} \\
L_{2new} &= \frac{L_{2prototype} * G_m}{F_{new} * Q} \\
C_{2new} &= \frac{C_{2prototype} * G_m * Q}{F_{new}} \\
L_{3new} &= \frac{L_{3prototype} * G_m * Q}{F_{new}} \\
C_{3new} &= \frac{C_{3prototype} * G_m}{F_{new} * Q}
\end{aligned} \tag{4.2}$$

As shown in the equations, the quality factor either multiplies or divides each passive element in the band pass filter circuit. For a Q of 20, the passive elements become those shown in table 4.3.

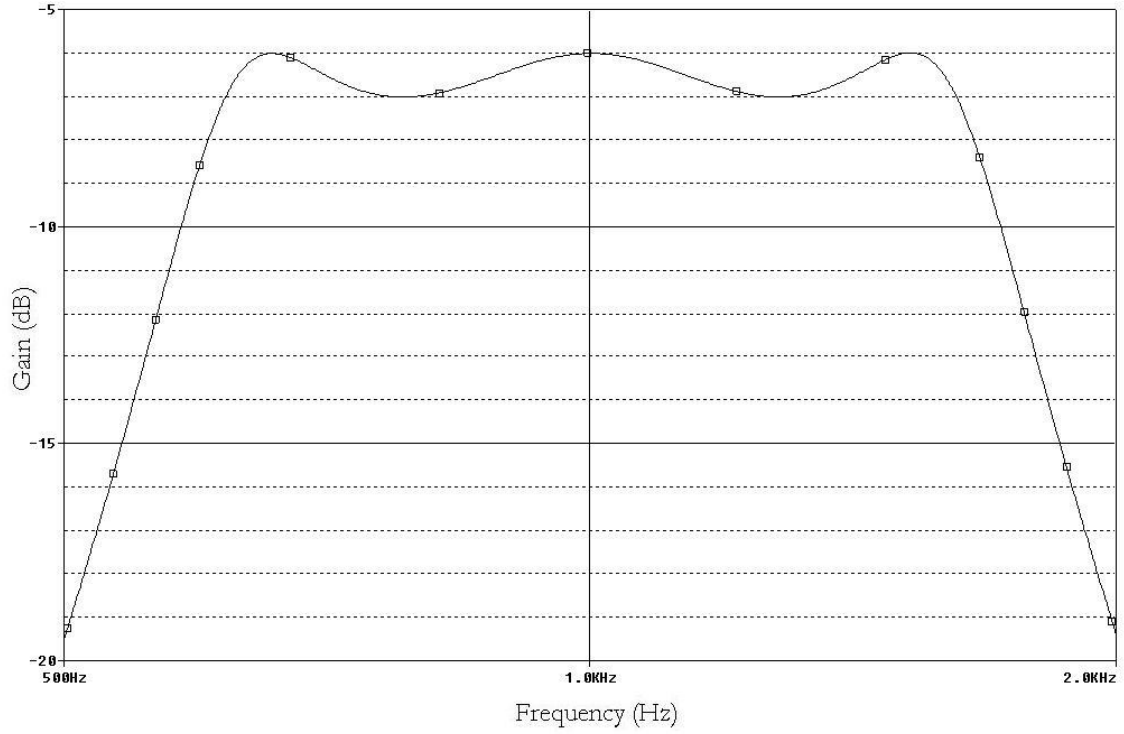


Figure 4.4: Third order Chebyshev band pass with $F_c = 1$ kHz, $Q=1$

Element	Capacitance
L1	422.6 pF
C1	0.258 pF
L2	0.519 pF
C2	210 pF
L3	422.6 pF
C3	0.258 pF

Table 4.3: Capacitor values for band pass filter with $Q=20$

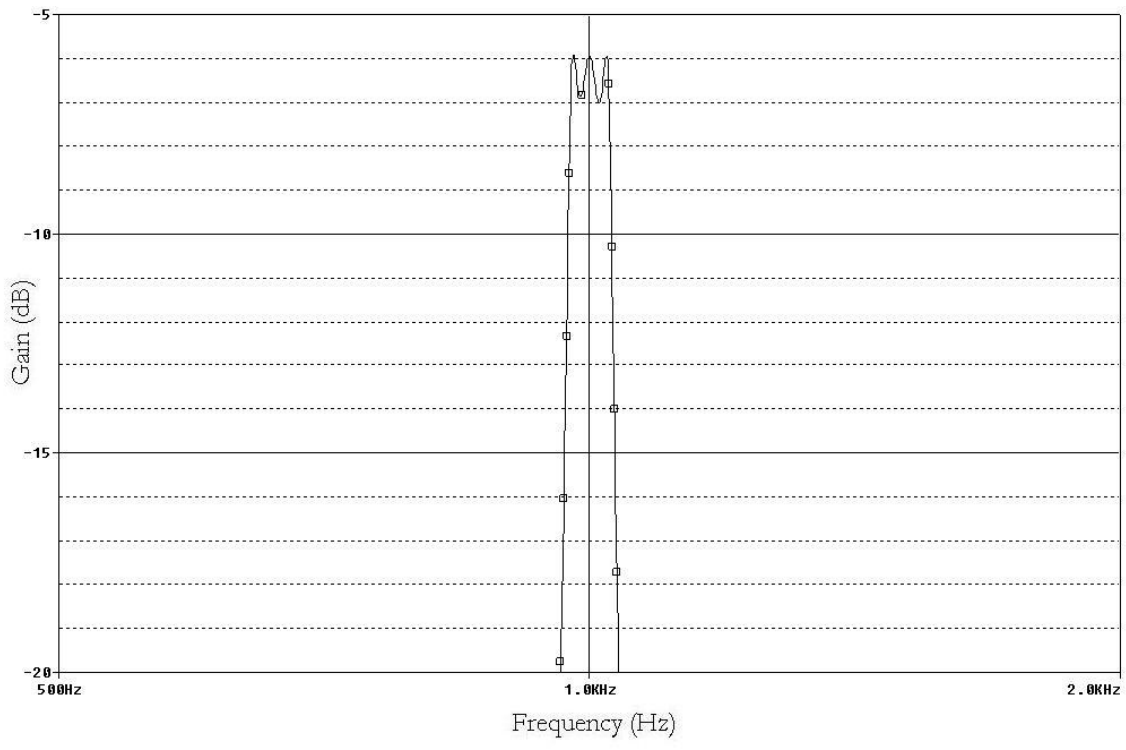


Figure 4.5: Third order Chebyshev band pass with $F_c = 1$ kHz, $Q=20$

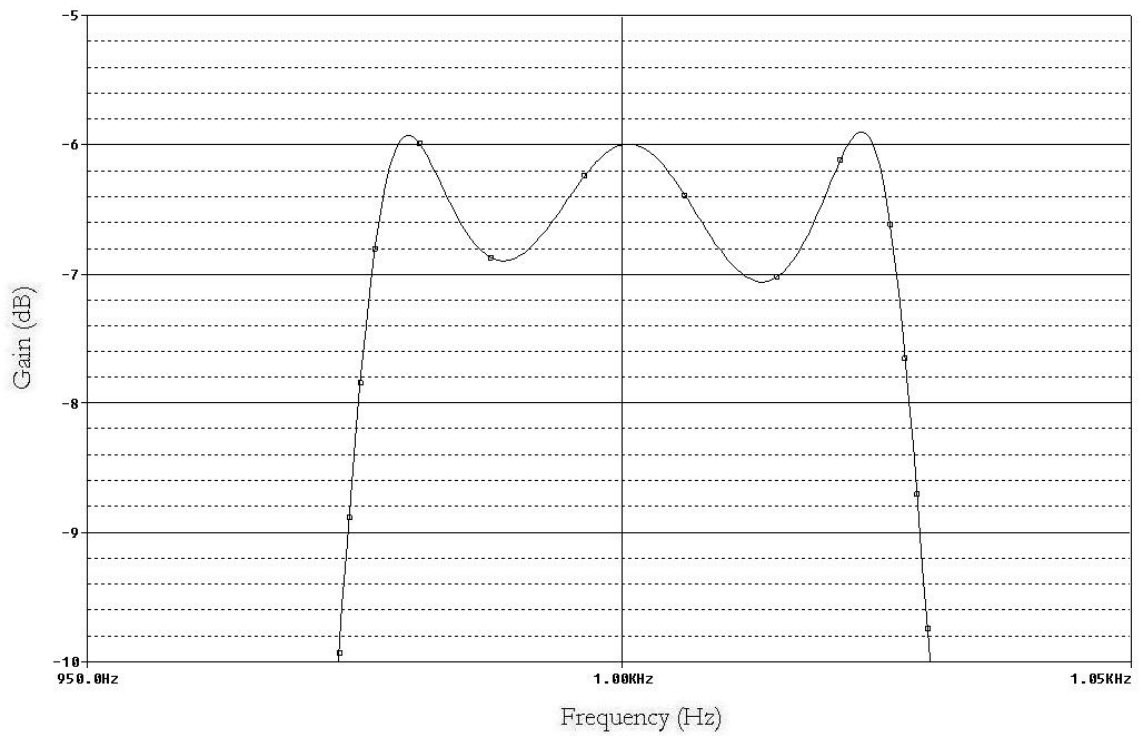


Figure 4.6: Exploded view of third order Chebyshev band pass filter with $F_c = 1$ kHz, $Q=20$

As clearly shown in table 4.3, increasing the quality factor means spreading out the capacitance values required by the circuit. Figure 4.5 shows the frequency response for the circuit with a quality factor of 20. The smaller bandwidth is very evident. Figure 4.6 shows the same simulation with an exploded view of the passband. Here, some of the non-ideal effects begin to show. A close inspection of Figure 4.6 reveals that the passband ripples are not exactly the same. This is caused by the relatively small values of capacitors needed to achieve a quality factor of 20. At smaller capacitance levels, the input capacitance of the OTA's become a factor in the transfer function. The fact that several OTA inputs are often connected to a single OTA output only serves to enhance the problem. At a Q of 20, the effect is minor. However, if the quality factor were increased, or the capacitors decreased the problem would escalate quickly.

As was the case in the low pass filter, the reference current can be changed to tune the filter center frequency. Figure 4.7 shows the resulting frequency response of the high quality factor filter with four different reference currents. Also as before, the tuning is quite linear. Figure 4.8 shows the tuning linearity by comparing reference current to center frequency of the band pass filter.

4.3 Implementation of Higher Order Filter

Due to their sharper roll off, higher order filters are desired in many systems. However, for many circuit topologies their design can be difficult. This often leads to unnecessarily large and complicated circuits. One of the important benefits of the

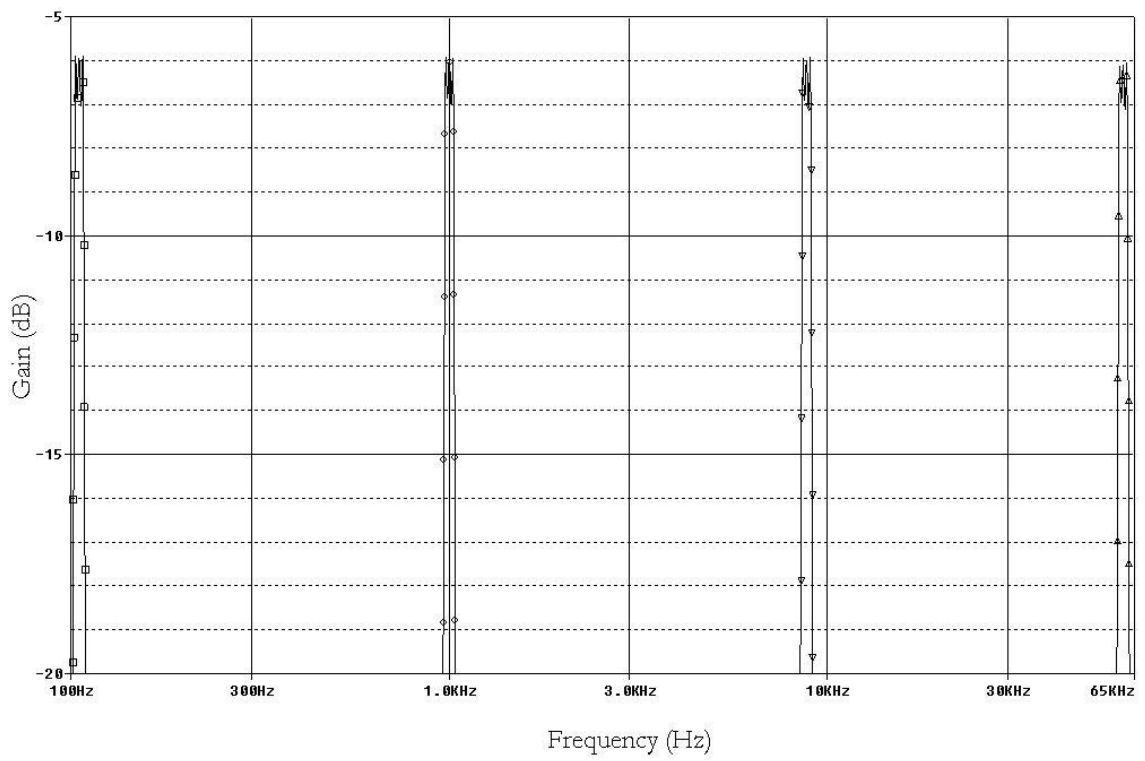


Figure 4.7: Third order Chebyshev band pass filter for four reference currents

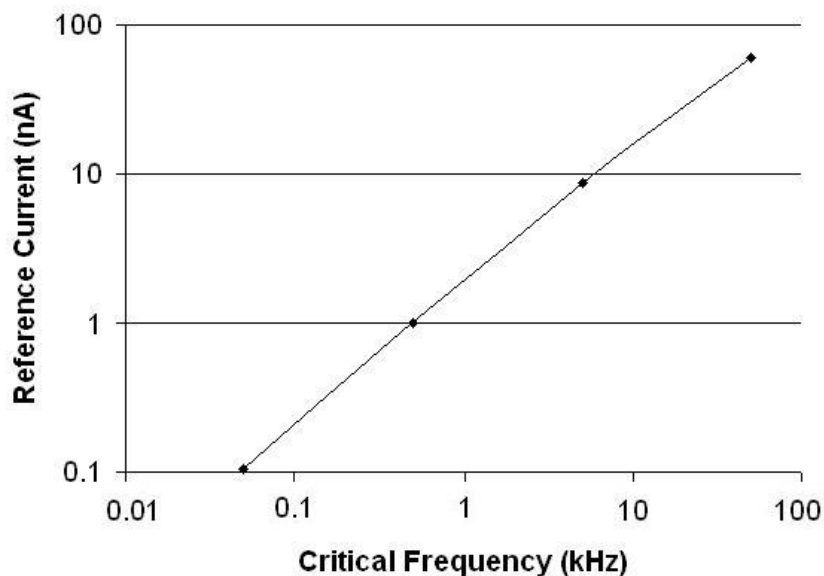


Figure 4.8: Reference current vs BPF center frequency

synthesis process presented in this paper is the ease of extension to high order transfer functions. To emphasize this concept, the previously designed 3^{rd} order Chebyshev band pass filter will be extended to a 5^{th} order one.

Figure 4.9 shows the minimum capacitance ladder circuit for a 5^{th} order band pass filter. Keeping the previously defined notation of currents through inductors and voltages across capacitors, the state equations describing Figure 4.9 are shown in equation set (4.3). Manipulating the equations to implement them using standard two and four input OTA designs, the OTA-C circuit is as shown in Figure 4.10. When compared to the equations and schematic of the 3^{rd} order filter designed in section 2.2, it is clear that the 5^{th} order design is merely an extension of the 3^{rd} order. This explains why the first few equations and devices are the same. The design of

Chebyshev filter with a quality factor of 10 results in the capacitor values of table 4.4. As mentioned previously, the capacitor values are scaled depending on the desired frequency range as well as the OTA transconductance.

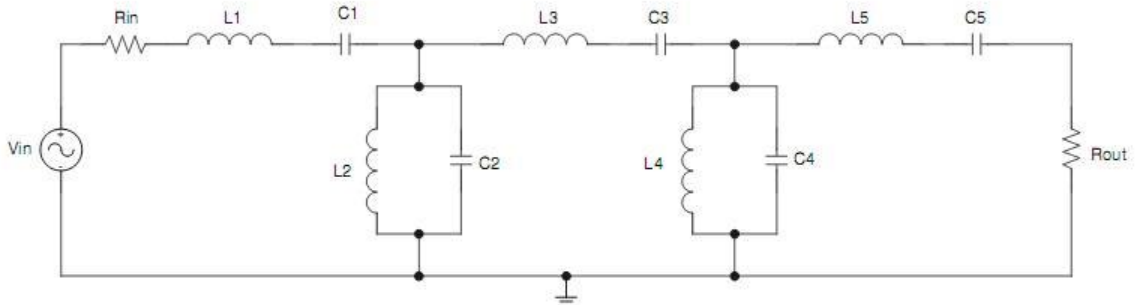


Figure 4.9: 5th order band pass filter ladder circuit

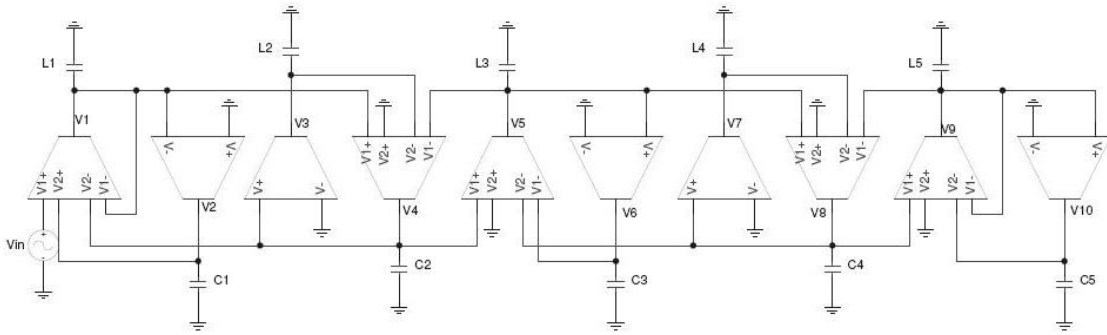


Figure 4.10: 5th order prototype Chebyshev BPF OTA implementation

$$\begin{aligned}
\dot{i}_1 &= \frac{1}{L_1}(V_{in} - i_1 R_{in} + v_2 - v_4) \\
\dot{v}_2 &= \frac{1}{C_1}(-i_1) \\
\dot{i}_3 &= \frac{1}{L_2}(v_4) \\
\dot{v}_4 &= \frac{1}{C_2}(i_1 - i_3 - i_5) \\
\dot{i}_5 &= \frac{1}{L_3}(v_4 - v_6 - v_8) \\
\dot{v}_6 &= \frac{1}{C_3}(i_5) \\
\dot{i}_7 &= \frac{1}{L_4}(v_8) \\
\dot{v}_8 &= \frac{1}{C_4}(i_5 - i_7 - i_9) \\
\dot{i}_9 &= \frac{1}{L_5}(v_8 - v_{10} - i_9 R_{out}) \\
\dot{v}_{10} &= \frac{1}{C_5}(i_9)
\end{aligned} \tag{4.3}$$

L1	339.4 pF
C1	0.745 pF
L2	1.46 pF
C2	173.5 pF
L3	477.1 pF
C3	0.53 pF
L4	1.46 pF
C4	173.5 pF
L5	339.4 pF
C5	0.745 pF

Table 4.4: Capacitor values for 5th order band pass filter with Q=10

Figures 4.11 and 4.12 clearly show the advantages of the higher order design. With the added roll off, quality factors can be reduced in many applications. This improvement comes at the expense of only five extra OTAs and their associated

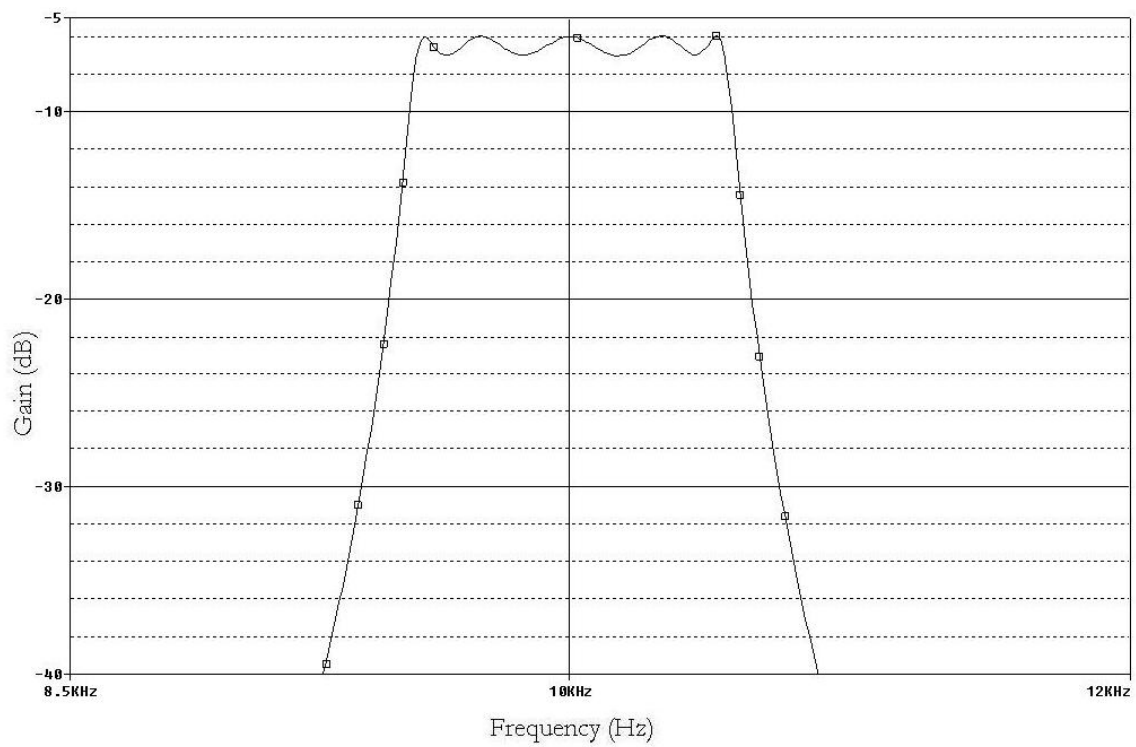


Figure 4.11: Fifth order Chebyshev band pass filter centered at 10 kHz

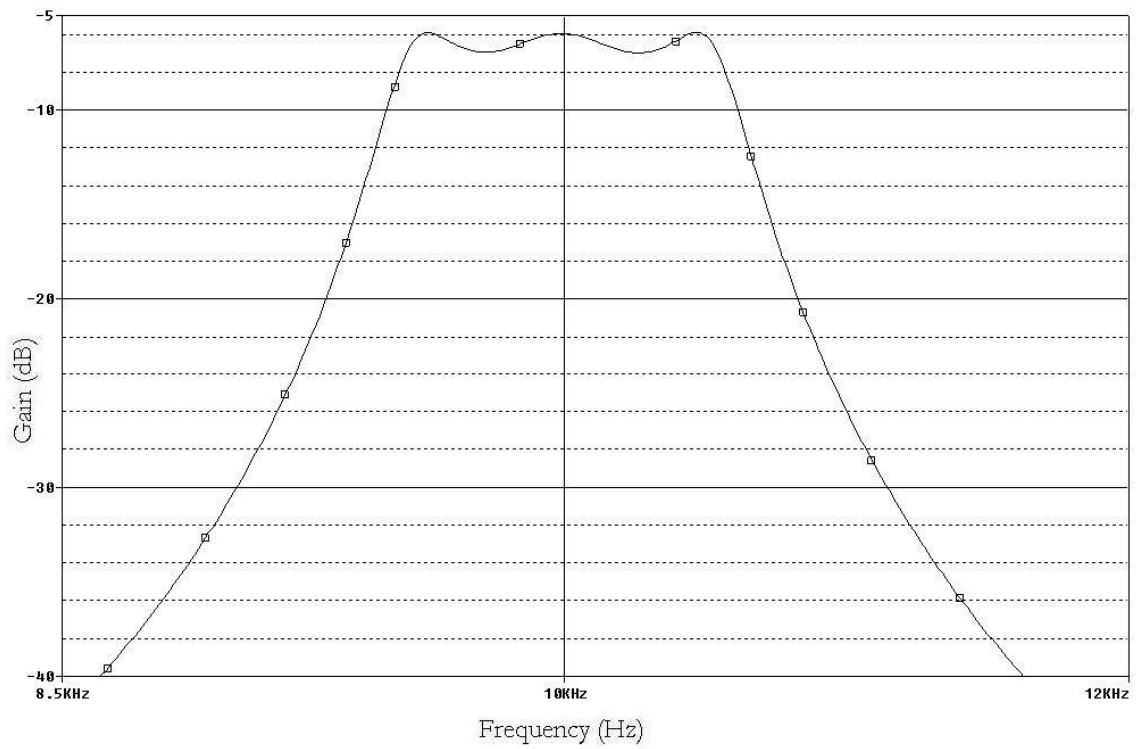


Figure 4.12: Third order Chebyshev band pass filter centered at 10 kHz

capacitances. Figure 4.13 shows the 5th order filter ranging from 1 kHz to 10 kHz. As shown, the shape is very consistent through the tuning range.

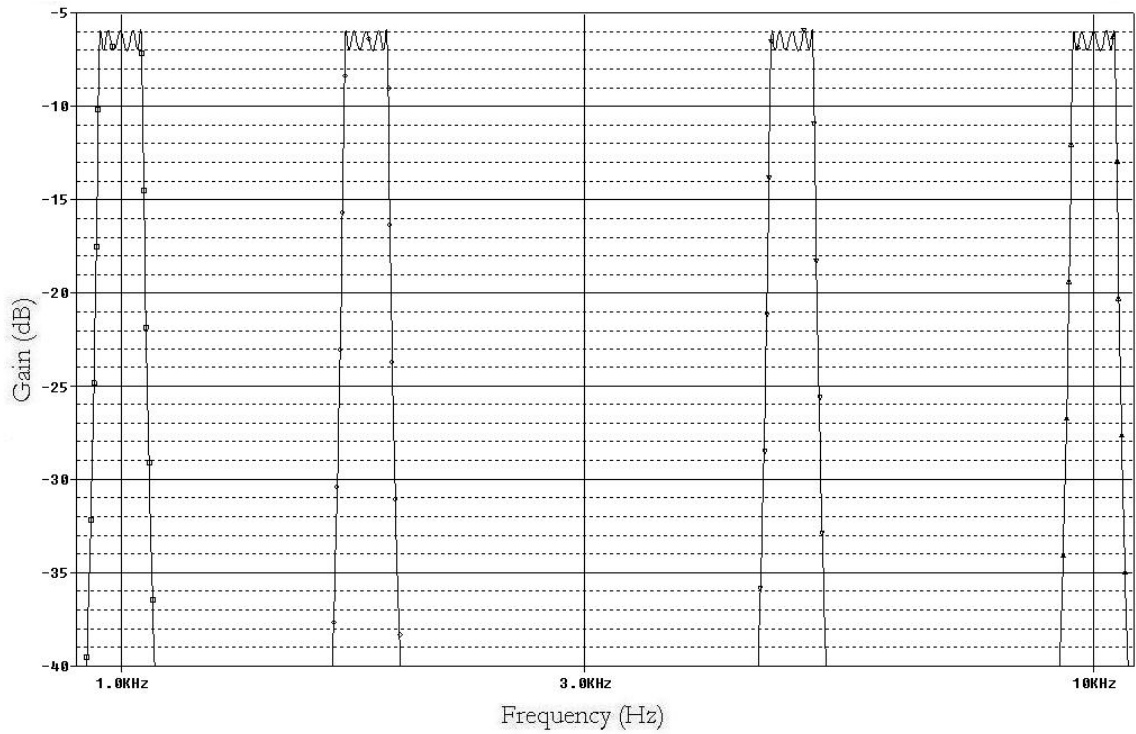


Figure 4.13: Fifth order Chebyshev band pass filter ranging 1 kHz to 10 kHz

CHAPTER 5

CONCLUSION

In this thesis, a convenient method of synthesizing OTA-C filters is presented. Any transfer function that can be implemented in a simple ladder circuit can be transformed into its OTA-C equivalent. Unlike other synthesis methods, it does not depend on a second order section or any other type of building block. This fact gives the designer more freedom as well as decreases the filter's sensitivity to component values. To emphasize this point, a 3rd order Chebyshev low pass filter and its bandpass transform were synthesized to their equivalent OTA-C circuit.

Using SPICE a prototype OTA is developed in 0.5 μm technology. Special care is taken to address those issues most important to filtering applications. Foremost, maintaining a large output resistance throughout the operating region is accomplished through the use of a mirrored cascode structure. To make it possible to tune the transconductance linearly, the biasing currents are kept low. Finally, the frequency response of the amplifier is improved by improving the current mirror used in the mirrored cascode design. The resulting amplifier is appropriate for use in filtering applications requiring high quality factors.

The prototype OTA developed throughout Chapter 3 was then substituted into the circuits from Chapter 2. In the case of the low pass filter, the results were almost identical to the ideal case. The implemented filter was capable of being tuned linearly from a critical frequency of 10 Hz to around 500 kHz using reference currents from

0.05 nA to 500 nA. Even higher critical frequencies can be obtained from the circuit, but the critical frequency tuning becomes less linear at higher reference currents. For a quality factor of 1, the band pass filter can have of a response as ideal as the low pass. However, things become more interesting as the quality factor increases. The filter implemented in section 4.2 can achieve a quality factor of 20 while the center frequency of the filter can be tuned linearly from 100 Hz to around 50 kHz. Although higher quality factors can be reached, trade offs must be made between capacitor sizes, frequency, and Q. As an example of the ease with which higher order filters can be implemented, a 5th order Chebyshev band pass filter was designed. Because of the much steeper roll off, quality factor constraints can often be reduced in filters of higher order. The results show a very versatile filter structure that can find use in many applications.

BIBLIOGRAPHY

- [1] R. D. Koller and B. M. Wilamowski, "A ladder Prototype Synthesis Algorithm,," *35th Midwest Symp. Circuits and Systems*, Washington, DC, USA, Aug. 9-12, 1992.
- [2] Robert D. Koller and Bogdan Wilamowski, "LADDER—A Microcomputer Tool for Passive Filter Design and Simulation," *IEEE Transactions on Education*, vol. 39, no. 4, Nov. 1996.
- [3] Bogdan M. Wilamowski and Ramraj Gottiparthi, "Active and Passive Filter Synthesis using MATLAB," *International Journal of Engineering Education*, vol. 21, no. 4, pp.561-571, 2005.
- [4] Rolf Schaumann, "Simulating Lossless Ladders with Transconductance-C Circuits," *IEEE Transactions on Circuits and Systems-II: Analog and Digital Signal Processing*, vol. 45, no. 3, Mar. 1998.
- [5] Edgar Sanchez-Sinencio, Randall L. Geiger, And H. Nevarez-Lozano, "Generation of Continuous-Time Two Integrator Loop OTA Filter Structures," *IEEE Transactions on Circuits and Systems*, vol. 35, no. 8, Aug. 1988.
- [6] Mehmet A. Tan And Rolf Schaumann, "Design of a General Biquadratic Filter Section with Only Transconductances and Grounded Capacitors," *IEEE Transactions on Circuits and Systems*, vol. 35, no. 4, Aug. 1988.
- [7] Chun-Ming Chang, Bashir M. Al-Hashimi, Yichuang Sun, and J. Neil Ross, "New High-Order Filter Structures Using Only Single-Ended-Input OTAs and Grounded Capacitors," *IEEE Transactions on Circuits and Systems-II: Express Briefs*, vol. 51, no. 9, Sept. 2004.
- [8] Yichuang Sun and J. Kel Fidler, "Structure Generation and Design of Multiple Loop Feedback OTA-Grounded Capacitor Filters," *IEEE Transactions on Circuits and Systems-I: Fundamental Theory and Applications*, vol. 44, no. 1, Jan. 1997.
- [9] Yichuang Sun, "Synthesis of Leap-Frog Multiple-Loop Feedback OTA-C Filters," *IEEE Transactions on Circuits and Systems Express Briefs*, vol. 53, no. 9, Sept. 2006.

- [10] A. Zeki and H. Kuntman, "Accurate and high output impedance current mirror suitable for CMOS current output stages," *Electronics Letters*, 5th June 1997 Vol. 33 No. 12
- [11] Kuo-Hsing Cheng, Chi-Che Chen, And Chun-Fu Chung, "Accurate Current Mirror with High Output Impedance," *Electronics, Circuits and Systems, 2001. ICECS 2001. The 8th IEEE International Conference on*, Volume 2, 2-5 Sept. 2001 Page(s):565 - 568 vol.2
- [12] Silva-Martinez, J., "Design issues for UHF OTA-C filter realizations," *Mixed-Signal Design, 2001. SSMSD. 2001 Southwest Symposium on*, 25-27 Feb. 2001 Page(s):93 - 98
- [13] Adut, J. and Silva-Martinez, J., "Cascode transconductance amplifiers for HF switched-capacitor applications," *Circuits and Systems, 2003. ISCAS '03. Proceedings of the 2003 International Symposium on*, Volume 1, 25-28 May 2003 Page(s):I-365 - I-368 vol.1
- [14] Anderson, W. Matthew, Wilamowski, Bogdan M., and Dundar, Gunhan; "Wide Band Tunable Filter Design Implemented in CMOS," *Intelligent Engineering Systems, 11th International Conference on*, June 29 2007-July 1 2007 Page(s):219 - 223
- [15] Milind Subhash Sawant, Jaime Ramirez-Angulo, Antonio. J. Lopez-Martn, and Ramon G. Carvajal "Wide gm Adjustment Range Highly Linear OTA with Programmable Mirrors Operating in Triode Mode," *2006 IEEE International Symposium on Circuits and Systems*, 21-24 May 2006 Page(s):4 pp.
- [16] Yunbin Deng, S. Chakrabartty, and G. Cauwenberghs "Three-decade programmable fully differential linear OTA," *2004 IEEE International Symposium on Circuits and Systems*, Volume 1, 23-26 May 2004 Page(s):I - 697-700.

APPENDICES

APPENDIX A

SPICE LEVEL 7 NMOS MODEL FOR AMIS 0.5 μm PROCESS

```

.MODEL CMOSN NMOS (                                LEVEL = 7
+VERSION = 3.1          TNOM = 27          TOX = 1.41E-8
+XJ = 1.5E-7           NCH = 1.7E17       VTH0 = 0.6394078
+K1 = 0.8797763       K2 = -0.101648     K3 = 22.7282152
+K3B = -9.4213761     W0 = 1E-8         NLX = 1E-9
+DVTOW = 0            DVT1W = 0          DVT2W = 0
+DVT0 = 2.7334674     DVT1 = 0.419695          DVT2 = -0.1437711
+U0 = 479.4186448     UA = 2.410464E-13   UB = 2.100688E-18
+UC = 2.161768E-12    VSAT = 1.549123E5          A0 = 0.593756
+AGS = 0.138164       B0 = 2.476574E-6          B1 = 5E-6
+KETA = -3.000619E-3  A1 = 1.257922E-4          A2 = 0.3989121
+RDSW = 1.447499E3    PRWG = 0.014654          PRWB = 0.0320564
+WR = 1               WINT = 2.627592E-7          LINT = 7.265689E-8
+XL = 1E-7            XW = 0              DWG = -2.390541E-8
+DWB = 1.036659E-9    VOFF = 0              NFACTOR = 1.1157256
+CIT = 0              CDSC = 2.4E-4          CDSCD = 0
+CDSCB = 0            ETA0 = 2.616252E-3          ETAB = -9.856187E-5
+DSUB = 0.0879772     PCLM = 1.4276648          PDIBLC1 = 1
+PDIBLC2 = 2.890383E-3 PDIBLCB = -0.0207482      DROUT = 0.9774041

```

+PSCBE1	= 6.226031E8	PSCBE2	= 1.380813E-4	PVAG	= 0
+DELTA	= 0.01	RSH	= 81.8	MOBMOD	= 1
+PRT	= 0	UTE	= -1.5	KT1	= -0.11
+KT1L	= 0	KT2	= 0.022	UA1	= 4.31E-9
+UB1	= -7.61E-18	UC1	= -5.6E-11	AT	= 3.3E4
+WL	= 0	WLN	= 1	WW	= 0
+WWN	= 1	WWL	= 0	LL	= 0
+LLN	= 1	LW	= 0	LWN	= 1
+LWL	= 0	CAPMOD	= 2	XPART	= 0.5
+CGD0	= 1.99E-10	CGSO	= 1.99E-10	CGBO	= 1E-9
+CJ	= 4.270492E-4	PB	= 0.9112977	MJ	= 0.4304805
+CJSW	= 3.220481E-10	PBSW	= 0.8	MJSW	= 0.1979137
+CJSWG	= 1.64E-10	PBSWG	= 0.8	MJSWG	= 0.1979137
+CF	= 0	PVTHO	= -0.051744	PRDSW	= 346.3408616
+PK2	= -0.0305149	WKETA	= -0.0230394	LKETA	= 4.606854E-3

APPENDIX B

SPICE LEVEL 7 PMOS MODEL FOR AMIS 0.5 μm PROCESS

```

.MODEL CMOSP PMOS (
LEVEL = 7
+VERSION = 3.1          TNOM = 27          TOX = 1.41E-8
+XJ = 1.5E-7           NCH = 1.7E17         VTH0 = -0.9362224
+K1 = 0.55078          K2 = 4.146308E-3       K3 = 9.6961154
+K3B = -0.3221286      W0 = 1E-8           NLX = 3.858149E-8
+DVTOW = 0             DVT1W = 0           DVT2W = 0
+DVTO = 2.273307      DVT1 = 0.46069       DVT2 = -0.081477
+U0 = 233.5715825      UA = 3.503118E-9     UB = 2.45786E-21
+UC = -4.49043E-11     VSAT = 2E5           A0 = 0.8357554
+AGS = 0.1592968       B0 = 8.972676E-7     B1 = 5E-6
+KETA = -1.126827E-3   A1 = 1.166646E-4     A2 = 0.3423346
+RDSW = 3E3            PRWG = -0.030906     PRWB = -0.0122687
+WR = 1                WINT = 2.418604E-7   LINT = 9.180742E-8
+XL = 1E-7             XW = 0                DWG = -1.773591E-8
+DWB = 2.843285E-8     VOFF = -0.0798059    NFACTOR = 0.7194077
+CIT = 0                CDSC = 2.4E-4         CDSCD = 0
+CDSCB = 0             ETA0 = 6.759168E-3    ETAB = -0.120809
+DSUB = 1              PCLM = 1.9549807     PDIBLC1 = 0.0840943
+PDIBLC2 = 4.767307E-3 PDIBLCB = -0.0470009 DROUT = 0.2679617

```

+PSCBE1	= 5.610155E9	PSCBE2	= 5.295303E-10	PVAG	= 0.1243898
+DELTA	= 0.01	RSH	= 105.3	MOBMOD	= 1
+PRT	= 0	UTE	= -1.5	KT1	= -0.11
+KT1L	= 0	KT2	= 0.022	UA1	= 4.31E-9
+UB1	= -7.61E-18	UC1	= -5.6E-11	AT	= 3.3E4
+WL	= 0	WLN	= 1	WW	= 0
+WWN	= 1	WWL	= 0	LL	= 0
+LLN	= 1	LW	= 0	LWN	= 1
+LWL	= 0	CAPMOD	= 2	XPART	= 0.5
+CGD0	= 2.28E-10	CGSO	= 2.28E-10	CGBO	= 1E-9
+CJ	= 7.130689E-4	PB	= 0.9618253	MJ	= 0.4965243
+CJSW	= 3.009822E-10	PBSW	= 0.99	MJSW	= 0.3379563
+CJSWG	= 6.4E-11	PBSWG	= 0.99	MJSWG	= 0.3379563
+CF	= 0	PVTH0	= 5.98016E-3	PRDSW	= 14.8598424
+PK2	= 3.73981E-3	WKETA	= -2.023716E-3	LKETA	= -6.019389E-3